Supported single-atom catalysts: synthesis, characterization, properties, and applications

Jing Liu, Benjamin R. Bunes, Ling Zang & Chuanyi Wang

Environmental Chemistry Letters

ISSN 1610-3653
Volume 16
Number 2

Environ Chem Lett (2018) 16:477-505
DOI 10.1007/s10311-017-0679-2

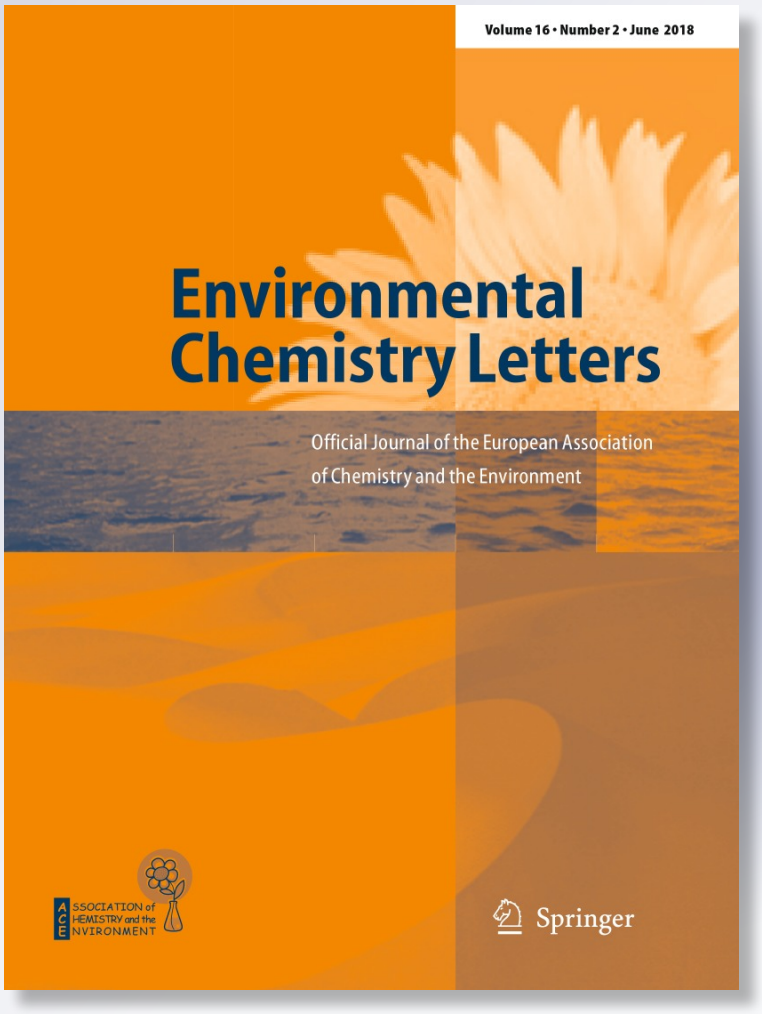

Springer

Environmental Chemistry Letters (2018) 16:477–505
https://doi.org/10.1007/s10311-017-0679-2

REVIEW

Supported single-atom catalysts: synthesis, characterization, properties, and applications

Jing Liu[1,2] · Benjamin R. Bunes[3,4] · Ling Zang[3] · Chuanyi Wang[1]

Received: 1 November 2017 / Accepted: 5 November 2017 / Published online: 22 November 2017

Abstract

In recent years, there has been a wide research in supported single-atom catalysts (SACs), which contain only isolated individual metal atoms dispersed on an appropriate support or coordinated with the surface atoms of the support. The SACs exhibit many fascinating characteristics including high activity, selectivity, and maximum atomic utilization. These characteristics arise from the low coordination status, quantum size effect, and the strong metal–support interaction, which have proved to be very powerful in many typical heterogeneous catalysis field including oxidation, hydrogenation, the water–gas shift reaction, methanol steam reforming, electrocatalysis, and photocatalysis. In this review, we summarized the recent progress in synthesis, characterizations, properties, and applications of SACs.

Keywords Catalysis · Single-atom · Oxidation · Reforming · Hydrogenation · Water–gas shift

Introduction

Supported metal catalysts, especially noble metals, such as Ru, Rh, Pt, Pd, Ni, Co, Au and Ag, are the most widely used in the field of heterogeneous catalysis (Yang and Tetsu 2005; Chen 2004; Enache 2006; Kunlun et al. 2015; Benjamin et al. 2006; Hao et al. 2008; Daniel et al. 2012; Edwards et al. 2005; Sakthivel et al. 2004). However, due to the high price and low natural abundance of such noble metals, they cannot meet the increasing demand. The utilization efficiency of noble metals in conventional supported catalysts tends to be low. In most cases, only the atoms on the surface of the nanoparticles act as active sites, while those inside the nanoparticles are spectators, which wastes the noble metals. For example, only 50% of metal atoms are used for catalysis when the metal is dispersed as 2-nm fine nanoparticles (Strizhak 2013). In the past several decades, enormous efforts have been devoted to maximizing the utilization efficiency of the supported noble metals (Xin-Bo et al. 2009; Crespo-Quesada et al. 2011; Mark et al. 2008; Lei et al. 2010). Any development that reduces the consumption of noble metals and increases their activity is of essential importance.

The research into reducing the size of the metal particles has attracted much attention over the past few years. As the size of one supported metal particle is reduced, a higher percentage of atoms are on the surface (a low coordination environment), combined with quantum size effect and strong metal–support interactions, these surface atoms become increasingly active to specific reactions. Accordingly, the most effective way to make use of each metal atom of supported metal catalysts is to reduce the metal size to well-defined, atomically distributed active centers, that is, SACs, which is the ultimate goal of fine dispersion. Zhang et al. prepared a practical Pt single-atom catalyst supported on iron oxide (Pt_1/FeO_x), which showed excellent stability and high activity for both CO oxidation and preferential

✉ Ling Zang
lzang@eng.utah.edu

✉ Chuanyi Wang
cywang@ms.xjb.ac.cn

1 Laboratory of Environmental Sciences and Technology, Xinjiang Technical Institute of Physics & Chemistry, and Key Laboratory of Functional Materials and Devices for Special Environments, Chinese Academy of Sciences, Ürümqi 830011, China

2 University of Chinese Academy of Sciences, Beijing 100049, China

3 Nano Institute of Utah and Department of Materials Science and Engineering, University of Utah, Salt Lake City, UT 84112, USA

4 Vaporsens Inc., 36 South Wasatch Drive, Salt Lake City, UT 84112, USA

oxidation of CO in H_2 (Qiao et al. 2011). However, as the particle size decreases, the surface energy will increase correspondingly, which leads to aggregation of the highly dispersed metal atoms. Therefore, the preparation of supported SACs is highly desirable.

The strong metal–support interactions play an essential role in preventing the aggregation, creating stable and finely dispersed SACs. Recently, various supports, such as metal oxide, metal, and two-dimensional (2D) materials (Lu et al. 2012), have been adopted to stabilize the single atoms through anchoring them on the surface (Chunlei et al. 2017; Sungeun et al. 2016; Matthew and Phillip 2016), inserting them into the framework (Xiaogang et al. 2016; Huan et al. 2015; Mao et al. 2014), or alloying them with support metal to form an alloyed SAC (Guang et al. 2015, 2017a, b; Matthew et al. 2017). Different synthetic methods, such as mass-selected soft landing (Lei et al. 2010), atomic layer deposition (ALD) (Gianvito et al. 2015), and wet chemistry (Melanie et al. 2013; Lin et al. 2013a, b; Guo et al. 2014), were applied to obtain atomic dispersion of the metal species on appropriate supports. All these efforts have brought about the successful synthesis of supported SACs confirmed by the advanced atomic resolution characterization techniques and theoretical calculation, and improved catalytic activity has been frequently reported. For example, Xiong et al. used the impregnation method to produce thermally stable Pt_1/CeO_2 SACs (Benjamin et al. 2016). Sun et al. synthesized individual Pt atoms anchored to graphene by the ALD technique. Such Pt SACs exhibited significantly improved catalytic activity in methanol electro-oxidation reactions (Sun et al. 2013). Toshima et al. prepared crown-jewel-structured Au/Pd nanocatalysts by a galvanic replacement reaction that atomically dispersed gold atoms on Pd clusters, which showed unprecedentedly high activity in glucose oxidation (Zhang et al. 2011). Our understanding of SAC has been further promoted in recent few years, including better understanding of sample preparations and characterizations, and the role of support, the strong metal–support interactions (Liu 2017), and the excellent properties of SACs have inspired many extensive investigations on their possible applications, such as oxidation (Kunlun et al. 2015; Joseph et al. 2014), hydrogenation (Guang et al. 2015; Aich et al. 2015), water–gas shift reaction (Yang et al. 2013a, b), methanol steam reforming (Xiang-Kui et al. 2014), electrocatalysis (Yantao et al. 2014), photocatalysis (Xiaogang et al. 2016), and others (Leilei et al. 2014).

SACs offer the opportunity to obtain new catalysts with enhanced selectivity, activity, and stability. Several excellent review articles have previously been published on the topics of SACs (Yang et al. 2013a, b; Flytzani-Stephanopoulos 2014; Liang et al. 2015; Zhu et al. 2017; Bing et al. 2017; Yang and Flytzani-Stephanopoulos 2017; Chithra et al. 2017; Liqiong et al. 2017; Ogino 2017; Parkinson 2017; Ting et al. 2017; Yong et al. 2017; Liang et al. 2017a, b). However, these articles were all published as overview or mini review, focusing on one of few aspects of SACs research. Therefore, it still remains highly demanded to publish a deep, extensive review covering the broad range chemistry topics of SACs, particulary the recent advances in materials and structure fabrication, and atomic-scale manipulation of property and function. Herein, we will focus on the recent controllable and facile preparation of SACs, advanced structure characterization technique, unique catalysis properties, and applications in various catalysis reactions. Besides, we will also provide deep understanding of recent progress, as well as possible challenges and breakthroughs coming in the near future on this rapidly advancing research field. Nevertheless, we hope this review will inspire more advancements in this area in the future.

Synthesis of SACs

Supports of SACs

Due to the huge surface free energy of single metal atoms, the deposited atoms are too mobile to aggregate to form large clusters. An appropriate support can effectively anchor the metal single atoms, prevent the aggregation, and create stable, finely dispersed SACs. Therefore, considerable attention in the SACs field has been paid to searching for appropriate supports. With the advanced characterization and computational modeling advances, a series of SACs have been successfully prepared, characterized, and tested, which show higher activity, selectivity, or both than their nanostructured counterparts. Many groups have experimentally and/or theoretically demonstrated that metal oxides, such as FeO_x (Lin et al. 2013a, b; Wei et al. 2014), CeO_2 (Sara et al. 2014; Ding et al. 2014), Al_2O_3 (Simon et al. 2007; Gao 2016), and ZnO (Xiang-Kui et al. 2014), are very promising supports for SACs, which may not only play a role to stabilize the single atoms, but also participate in reactions. In addition, the single-atom of one metal can be stabilized on the surface of another metal in the form of alloying, for instance, Pd single atoms on Cu (Guang et al. 2017a, b), Ag (Aich et al. 2015), or Au (Kesavan et al. 2011) surfaces. Beside traditional metal oxides and metals, attention has also been directed to 2D materials, which possess excellent physical and chemical properties. Many 2D materials, such as graphene (Huan et al. 2015), graphyne (Ma et al. 2015), graphitic (Zhang et al. 2013), N-doped carbon nanofibers (N-CNFs) (Dmitri et al. 2016), graphitic carbon nitride (g-C_3N_4) (Gao et al. 2016), single-layer hexagonal BN (h-BN) (Mao et al. 2014), C_2N (Ma et al. 2016), MoS_2 (Du et al. 2015), $SrTiO_3$ (Wang et al. 2014a, b), Ti_2CO_2 (Zhang et al. 2016a, b, c), and transition metal phthalocyanine monolayer sheets (TM-Pc) (Wang

et al. 2015a, b, c), have been investigated as supports for the SACs. Other materials, such as TiC (Sungeun et al. 2017), TiN (Sungeun et al. 2016), zeolites (Lu et al. 2012), phosphomolybdic acid (PMA) (Zhang et al. 2016a, b, c), ion-exchange resin (Leilei et al. 2014), metal organic framework (MOF) (Zhang et al. 2016a, b, c), and carbon nanotubes (CNTs) (Corma et al. 2015), were also used as substrates for the SACs. We will discuss below several supports that have been utilized to anchor metal single atoms. Table 1 provides a partial list of the supports for producing supported SACs.

Table 1 Partial list of the supports for supported SACs

Supports	Examples	References
Metal oxide	A_1/FeO_x (A = Ir, Pt, Au, Rh, Pd, Co, Cu, Ru, Ni, Ti), B_1/CeO_2(B = Au, Ru, Pt), $Pt_1/Au_1/ZnO$, Pd_1/TiO_2, Pt_1/WO_x, Pt_1/α-Al_2O_3, Pt_1/γ-Al_2O_3, Rh_1/γ-Al_2O_3, C_1/θ-Al_2O_3(C = Ni, Pt, Pd, Cu, Au, Ag), Au_1/ThO_2, Rh/CoO, Au_1/Co_3O_4, Ag/MnO_2, Mo_1/SiO_2	Qiao et al. (2011, 2015a, b) Matthew and Phillip (2016), Melanie et al. (2013), Lin et al. (2013a, b, 2015), Xiang-Kui et al. (2014), Wei et al. (2014), Sara et al. (2014), Ding et al. (2014), Gao (2016), Liang et al. (2014, 2016), Fengyu et al. (2015), Li et al. (2016), Dvořák et al. (2016), Narula et al. (2014), Narula and Stocks (2012), Peterson et al. (2014), Tang et al. (2016), Figueroba et al. (2016), Long et al. (2016), Wang et al. (2015a, b, c, 2016a, b, c), Gai et al. (2016), Shi et al. (2016), Ghosh and Nair (2013), Zhiwei et al. (2012), Xing et al. (2014), Lang et al. (2016), Matsubu et al. (2015), Jinxia et al. (2017), Yan et al. (2017a, b), Xinjiang et al. (2017), Hongling et al. (2017), Sun et al. (2017), Yang et al. (2017), Liu et al. (2017a, b, c), Ewing et al. (2016)
Metal	Pt–Cu, Pd–Cu, Pd–Ag, Pd–Au, Ni–Au,	Guang et al. (2015, 2017a, b), Matthew et al. (2017), Aich et al. (2015), Leilei et al. (2014), Kesavan et al. (2011), Wang et al. (2016a, b, c), Kyriakou et al. (2012), Cao et al. (2014, 2015a, b), Lucci et al. (2015, 2016), Songhai et al. (2012), Zhang et al. (2014), Jirkovsky et al. (2011), Cheng et al. (2016a), Liu et al. (2016a, b)
Graphene	M_1/graphene (M = Fe, Au, Pt, Ir, Pd, Rh, Ru, Co, In, Si)	Huan et al. (2015), Sun et al. (2013), Ma et al. (2015), Wang et al. (2012, 2014a, b), Fei et al. (2015), Wu et al. (2015), Cheng et al. (2016a, b), Stambula et al. (2014), Xu et al. (2017), He and Jagvaral (2017), Liu et al. (2017a, b, c), Qiu et al. (2015)
Graphitic	Nb_1/graphitic	Zhang et al. (2013)
g-C_3N_4	Pd–Pt/g-C_3N_4	Xiaogang et al. (2016), Gianvito et al. (2015), Gao et al. (2016), Zupeng et al. (2017), Huang et al. (2017)
C_2N	X_1/C_2N (X = Sc, Ti, V, Cr, Mn)	Ma et al. (2016)
Graphdiyne	Sc_1/graphdiyne, Ti_1/graphdiyne	Ma et al. (2015), Lin (2016)
BP	ZnN_x/BP	Ping et al. (2017)
h-BN	N_1/h-BN (N = Cu, Fe, Ag, Au, Pt, Rh, Pd, Co, Ir)	Mao et al. (2014), Gao et al. (2013), Lin et al. (2013a, b), Zhao et al. (2011), Liu et al. (2014, 2015), Lu et al. (2017)
MoS_2	Pt_1/MoS_2	Du et al. (2015), Alex et al. (2016), Shi (2017)
$SrTiO_3$	$Ni_1/SrTiO_3$	Wang et al. (2014a, b)
Ti_2CO_2	Ti_1/Ti_2CO_2	Zhang et al. (2016a, b, c)
TiC	Pt_1/TiC	Sungeun et al. (2017), Seoin and Yousung (2017)
TiN	Pt_1/TiN	Sungeun et al. (2016), Sungeun et al. (2017), Seoin and Yousung (2017), Zhang et al. (2012a)
TM-Pc	M-Pc(M = Sc, Ti, V, Mn, Fe, Co, Ni, Cu, Zn, Cr,)	Wang et al. (2015a, b, c), Deng et al. (2013), Li et al. (2014)
PMA	Pt_1/PMA	Zhang et al. (2016a, b, c)
zeolites	Au_1/zeolite NaY, Pt_1/zeolite KLTL	Lu et al. (2012), Joseph et al. (2014)
Ion-exchange resin	Au–Pd/resin	Leilei et al. (2014)
CNFs	Pt_1/N-CNFs, Pd_1/N-CNFs,	Dmitri et al. (2016)
CNTs	Au_1/MWCNTs, Pd_1/N-CNTs.	Corma et al. (2015), Rosa et al. (2015)
MOF	Co_1/MOF-525	Zhang et al. (2016a, b, c)
Mo_2C	Pt_1/Mo_2C	Li et al. (2017)
C/N	Co–N–C, Fe–N–C	Liu et al. (2016a, b, 2017a, b, c), Li (2016)

Metal oxides

A single metal atom can substitutionally replace a surface cation of a metal oxide support then the metal atom may be strongly anchored due to its interaction with the neighboring oxygen anions (Albert et al. 2014). For instance, Zhang et al. prepared the Pt single-atom catalyst supported on iron oxide (Pt_1/FeO_x) (Qiao et al. 2011). High-angle annular dark-field scanning transmission electron microscopy (HAADF-STEM) images clearly revealed that isolated Pt atoms occupy exactly the positions of the Fe atoms. The more vacant *d* orbitals of the single Pt atoms, because of the electron transfer from single Pt atoms to the FeO_x surface, are responsible both for the strong binding and stabilization of individual Pt atoms and for providing positively charged Pt atoms, which ultimately account for the excellent catalytic activity of the Pt_1/FeO_x SAC. Inspired by the discovered highly active CO oxidation catalyst Pt_1/FeO_x (Qiao et al. 2011), Chen et al. systemically prepared various SACs M_1/FeO_x (M = Au, Rh, Pd, Co, Cu, Ru, and Ti) (Fengyu et al. 2015). The systems examined have very high stability (higher than or comparable to the Pt_1/FeO_x), as indicated by the strong binding energies and high diffusion barriers of the single metal atoms on the FeO_x support. The supported SAC $Pt_1/Au_1/ZnO$ was also reported by Li and co-workers (Xiang-Kui et al. 2014). The HAADF-STEM images showed that single Pt and Au atoms located on the Zn columns of the ZnO as shown in Fig. 1. The stability of $Pt_1/Au_1/ZnO$ can be explained that the observed single Pt or Au atoms are anchored onto the corresponding Zn vacancy positions. Density functional theory (DFT) calculations revealed that the catalysis of the single precious metal atoms together with coordinated lattice oxygen stems from its stronger binding toward the intermediates, lowering reaction barriers, changing on the reaction pathway, enhancing the activity.

Studies also confirmed the stabilization of single atoms by the surface defect of the metal oxide supports. Dvořák et al. (2016) showed the SAC Pt_1/CeO_2. Pt single atoms on CeO_2 were stabilized by the most ubiquitous defects on solid surfaces—monoatomic step edges (Fig. 2). Pt segregation at steps leaded to stable dispersions of single Pt^{2+} ions in planar PtO_4 moieties incorporating excess O atoms and contributing to oxygen storage capacity of CeO_2. Ceria surfaces provided a limited amount of low coordinated surface sites where Pt^{2+} ions could adsorb and remain stable in real applications. The step edges may represent a common type of adsorption sites providing stabilization for monodispersed metal atoms and ions in any oxide-supported SACs.

Metal

Single atoms can be also stabilized by anchoring on the surface of another metal in the form of an alloy. Generally speaking, a catalytically active metal is atomically dispersed in the surface layer of a more inert host metal. The more active of the two components is present in the surface of the host metal at very low content. Atoms of the more active component are thermodynamically more stable when surrounded by the host metal such that no dimers or trimers are present at low coverage. The single-atom alloys offer a means to both temper the reactivity of a very active element and to design catalysts with very small amounts of the precious metal. From a practical

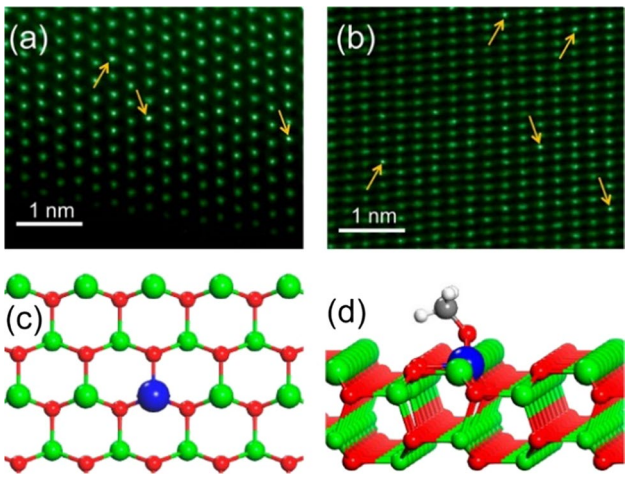

Fig. 1 HAADF-STEM images of ZnO nanowires with embedded Pt (**a**) and Au (**b**) atoms (indicated by the yellow arrow), respectively. **c** Schematic structure for $Pt_1/Au_1/ZnO$ (top view) and **d** $Pt_1/Au_1/ZnO$ with adsorbed CH_3O^* (side view). The blue, green, red, gray, and white spheres represent Pt_1/Au_1, Zn, O, C, and H atoms, respectively. Adapted from Xiang-Kui et al. (2014)

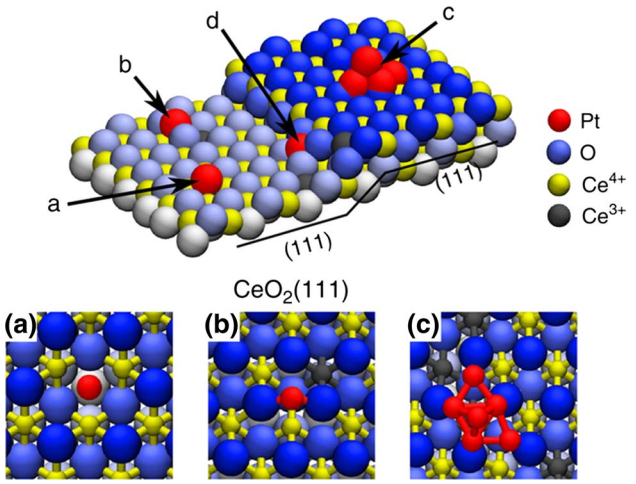

Fig. 2 Pt adsorption sites on the CeO_2 (111) surface obtained from DFT calculations. **a** Pt adatom in a surface O vacancy, **b** on the stoichiometric CeO_2 (111) terrace and **c** supported Pt_6 cluster. Adapted from Dvořák et al. (2016)

application standpoint, the small amounts of precious metal required to produce single-atom alloys generate a very attractive alternative to most traditional bimetallic catalysts.

A series of Ag alloyed Pd SACs, possessing only ppm levels of Pd, supported on silica gel were prepared and applied to the selective hydrogenation of acetylene in an ethylene-rich stream under conditions close to the front end employed by industry (Guang et al. 2015). High acetylene conversion and simultaneous selectivity to ethylene were attained over a wide temperature window, surpassing an analogous Au alloyed Pd single-atom system (Pei et al. 2014). By locating the isolated Pd atoms on a Cu surface, the energy barrier to both hydrogen uptake on and subsequent desorption from the Cu metal surface was lowered (Kyriakou et al. 2012). Minority Pd atoms (1 wt%) on a Cu surface activate hydrogen, which then populates the bare Cu areas (99%) where it is weakly bound and effective for hydrogenation, yielding a bifunctional surface with different regions facilitating different steps in the reaction. Pd–Ag alloy catalysts with very dilute amounts of Pd have also been studied (Aich et al. 2015). The extended X-ray absorption fine structure spectroscopy (EXAFS) results demonstrated that when the content of Pd was as low as 0.01 wt%, Pd was completely dispersed as isolated single atoms in Ag nanoparticles. The activity for the hydrogenation of acrolein was improved by the presence of these isolated Pd atoms due to the creation of sites with lower activation energy for H_2 dissociation (Fig. 3).

2D materials

Besides metal oxides and metals, a significant amount of attention has been directed toward 2D materials as the supports of SACs, such as graphene (Huan et al. 2015), graphyne (Wu et al. 2015), graphitic (Zhang et al. 2013), g-C_3N_4 (Gao et al. 2016), h-BN (Lin et al. 2013a, b), C_2N (Ma et al. 2016), MoS_2 (Du et al. 2015), $SrTiO_3$ (Wang et al. 2014a, b), Ti_2CO_2 (Zhang et al. 2016a, b, c), and transition metal phthalocyanine monolayer sheets (TM-Pc) (Deng et al. 2013), which have been used as promising catalyst supports for their large specific surface areas, and electronic and thermal properties, which play an important role in activity enhancement of catalysts.

Results indicate that the single metal atom supported by defective graphene present enhanced catalysis (Sun et al. 2013; Wang et al. 2012; Longhua et al. 2009; Machado and Serp 2012). For example, Lu et al. reported individually dispersed Pd on graphene (Huan et al. 2015). HAADF-STEM images and X-ray absorption near edge spectroscopy (XANES) both confirmed that isolated Pd single atoms dominantly existed on the graphene support. The SAC Pd_1/graphene was prepared by a process of anchor sites creation and selection. As shown in Fig. 4, the dominate oxygen species remaining on the graphene support was phenolic oxygen. The isolated phenol groups were the active sites for anchoring the palladium hexafluoroacetylacetate ($Pd(hfac)_2$) precursor, by forming –O–Pd-hfac surface species and H-hfac gaseous product. Next, isolated Pd single atoms are formed after removing the rest hfac ligand by exposure to formalin. In selective hydrogenation of 1, 3-butadiene, the single-atom Pd_1/graphene catalyst showed nearly 100% selectivity

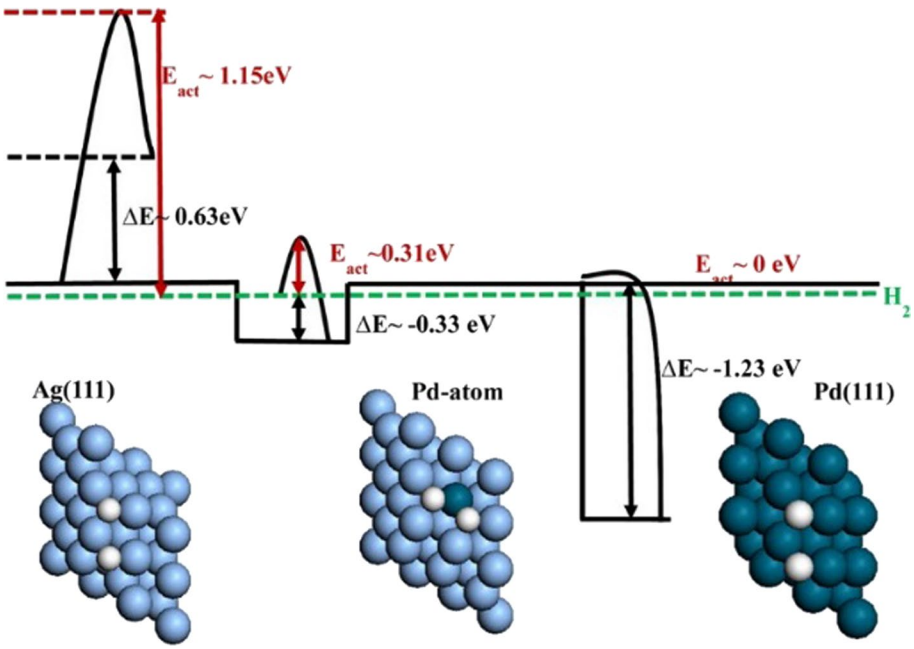

Fig. 3 Potential energy diagram showing how the Pd single-atom alloys surface has an effect on the energies compared to those for the Ag (111) and Pd (111) surface. Dissociation of H_2 (white) on Ag (111) (blue) is a significantly activated process. On Pd (111) (green), H_2 dissociation has practically no barrier; however, the binding energy of adsorbed atoms is high. For the Pd/Ag (111) single-atom alloys surface, the dissociation barrier is reduced and binding energy of hydrogen is decreased allowing dissociated hydrogen to get spilled over to the Ag surface (E_{act} = activation energy, ΔE = reaction enthalpy). Adapted from Aich et al. (2015)

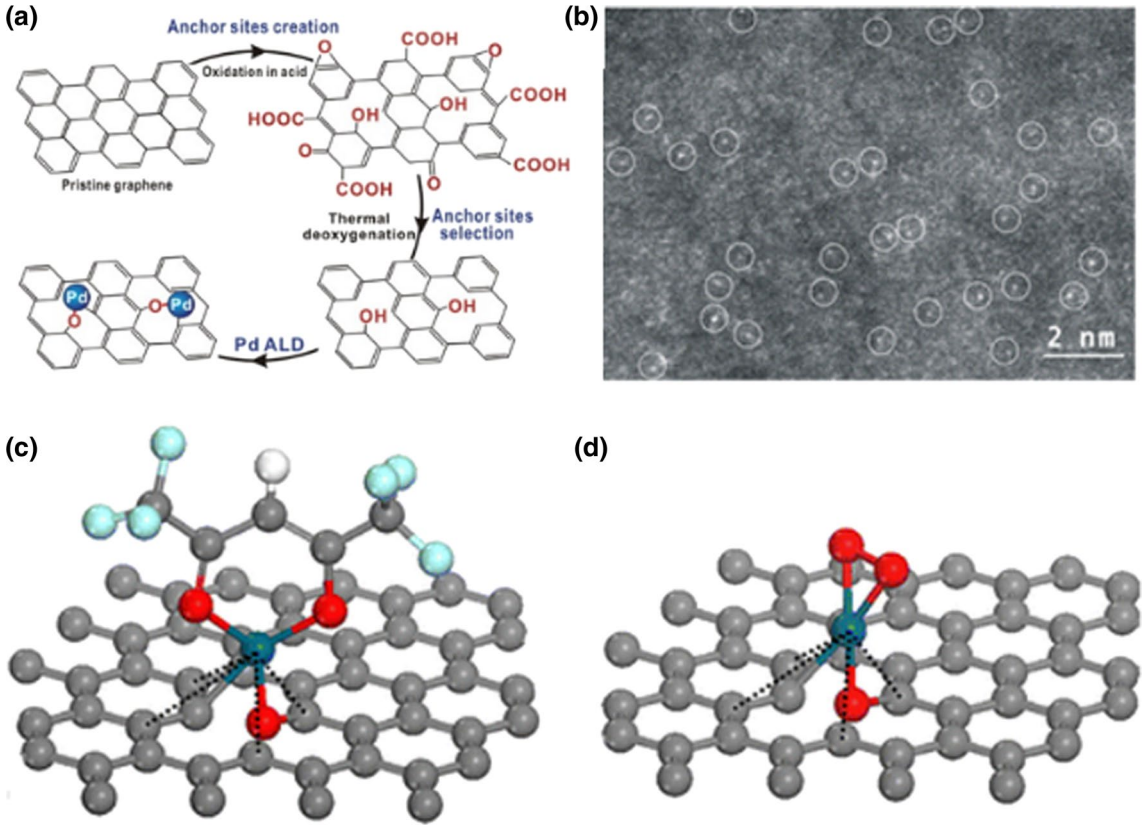

Fig. 4 **a** Schematic illustration of single-atom Pd_1/graphene catalyst synthesis via a process of creation and selection of anchor sites and ALD of Pd on pristine graphene. **b** Representative HAADF-STEM images of atomically dispersed Pd atoms highlighted by the white circles. Schematic models of **c** Pd-hfac/graphene and **d** Pd_1/graphene, where the balls in gray, red, dark cyan, light blue, and white represent carbon, oxygen, palladium, fluorine, and hydrogen atoms, respectively. The Pd-C_2 coordination is indicated by the black, dashed line in (**c**, **d**). Adapted from Huan et al. (2015)

to butene and 95% conversion at a mild reaction condition of about 50 °C. More importantly, excellent durability against deactivation via either aggregation of metal atoms or carbonaceous deposits during a total reaction time of 100 h on stream was achieved.

Beside graphene, many other 2D carbon nanomaterial-based SACs are investigated, such as Fe_1/graphyne (Ma et al. 2015), Ni/graphitic (Zhang et al. 2013), Pt_1/N-CNFs, and Pd_1/N-CNFs (Dmitri et al. 2016). Graphyne can be a good support candidate for synthesis of SACs without requiring the creation of monovacancies by high-energy atom/ion beam. The potential of graphyne as substrate materials for noble metal (Au, Pt, Ir, Pd, Rh, and Ru) SACs has been systematically investigated (Ma et al. 2015). It was found that the adsorption of most considered noble metal single atoms is very strong at the hollow site above the center of the acetylenic ring of the graphyne sheet and their diffusion away from this site toward neighboring sites is rather difficult, which enables realization of well-ordered and uniformly distributed noble metal single-atom catalysts on graphyne (Fig. 5a). Wu et al. (2015) reported the formation of a graphyne-supported single Fe atom catalyst (Fe_1/graphyne). Fe atoms bond strongly to graphyne and have a relatively high diffusion barrier, which prevents the formation of Fe clusters. Zhang et al. (2013) reported a Ni-carbon structure for catalyzing the oxygen reduction reaction. A large number of single Ni atoms trapped in graphitic layers, which were found to be incorporated into onion-like carbon shells surrounding ~ 1.6-nm Ni carbide cores. Experimental studies have unambiguously confirmed that O_2 can penetrate into the graphitic layers and react at specific doping sites (Fig. 5b). The large number of graphitic defects improves O_2 permittivity and possibly has a role as catalytically active sites for O_2 reduction. Dmitri et al. (2016) reported that single Pd^{2+} atoms supported on N-doped graphene-like carbon could be the active sites for the formic acid decomposition reaction with high selectivity (Fig. 5c). The single metal atom is coordinated by a pair of pyridinic nitrogen atoms at the edge of N-functionalized carbon sheets. The chelate binding provides an ionic/electron-deficient state of these atoms that prevents the aggregation and then leads to excellent stability under the reaction conditions.

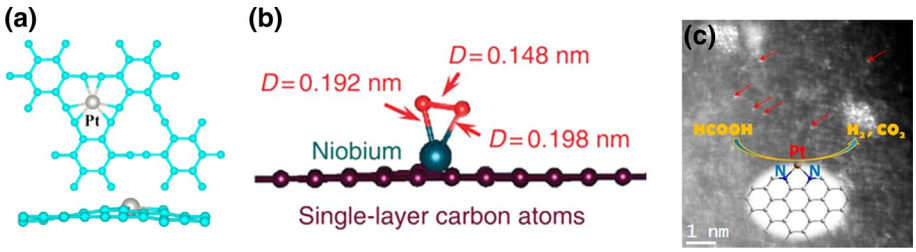

Fig. 5 **a** Top and side views of the geometric structures of Pt_1/graphyne. **b** Geometric arrangement of adsorbed O_2 on the single Ni site support on the graphitic layers. **c** Formic acid decomposition reaction by single Pt supported on N-doped graphene-like carbon. Adapted from Ma et al. (2015), Zhang et al. (2013) and Dmitri et al. (2016)

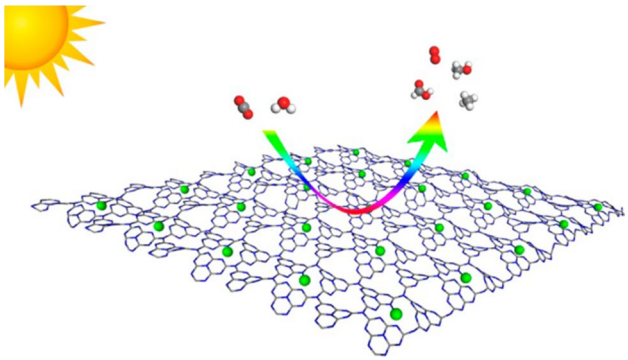

Fig. 6 Schematic illustration of CO_2 reduction by Pd_1/g-C_3N_4 and Pt_1/g-C_3N_4. The balls in green, gray, red, and white represent Pd/Pt, carbon, oxygen, and hydrogen atoms, respectively. Adapted from Gao et al. (2016)

g-C_3N_4 is a promising, active, stable, and metal-free photocatalyst, which has also been reported to be an excellent substrate for supporting catalysts (Ma et al. 2012). The N/C-coordinating framework formed by the unique tri-s-triazine structure facilitates the binding or intercalation of exotic atoms into the matrix of g-C_3N_4, providing a potential scaffold for firmly trapping the highly active single metal atoms. It has been shown experimentally and theoretically that g-C_3N_4 can tightly trap the single Pd atoms into its sixfold N-coordinating cavity and the resulting SACs surpass the activity of conventional heterogeneous catalysts based on nanoparticles while maintaining an outstanding degree of product selectivity. Du et al. reported the single atoms of palladium and platinum supported on g-C_3N_4, namely Pd_1/g-C_3N_4 and Pt_1/g-C_3N_4 (Gao et al. 2016). The as-designed SACs exhibit excellent activity in CO_2 reduction. The sixfold cavity of g-C_3N_4 is the most stable site for the deposition of Pd and Pt atoms as shown in Fig. 6. There is significant charge transfer between the metal atoms and the neighboring pyridinic nitrogen atoms for Pd_1/g-C_3N_4 and Pt_1/g-C_3N_4, indicating a strong interaction between the lone pair electrons of the neighboring pyridinic nitrogen atoms and the isolated metal atoms. Similar to g-C_3N_4, C_2N monolayer as SAC supports for the 3*d* transition metal (TM) (Sc to Zn) has been studied (Ma et al. 2016). The calculated energies indicate that the early 3d TM (Sc, Ti, V, Cr, and Mn)-embedded C_2N monolayers are the very promising SACs, because these TM single atoms can be strongly trapped in the cavity of the C_2N monolayer and exist in the isolated form.

Drawing considerable attention recently, h-BN has planar structure such as graphene but with different chemical and physical properties. Due to the different electronegativities of B and N, h-BN is more ionic, leading the interaction and charge transfer with deposited metal atoms to be different from those with graphene. Various defects, such as vacancies and boundaries, exist in the as synthesized h-BN sheets. The existence of these defects over h-BN provides a new platform for fabrication of finely dispersed single metal atom catalysts. By means of first-principles computation, metal (Cu, Ag, Au, Pt, Rh, Pd, Fe, Co, and Ir)-doped hexagonal boron nitride nanosheets (h-BNNSs) have been systematically studied (Fig. 7) (Lin et al. 2013a, b). The strong interaction between the metal atoms and defect sites in h-BNNS, such as the B vacancy and N edge, suggests that metal-doped h-BN nanosheets (M-BNNSs) should be stable under high temperatures. Liu and his collaborators reported the Pt atoms stabilized by B vacancies on h-BN by first-principles-based calculations (Liu et al. 2015). Pt atoms use Pt-d and Pt-*sp* states to interact with the localized defect states on B vacancy. This interaction is as strong as ~ 4.40 eV, which not only prohibits the diffusion and aggregation of stabilized Pt atoms, but also shifts some Pt-*d* states to stand at the E_F. These upshifted dangling Pt-*d* states contribute to the enhanced reactivity and catalytic performance of Pt atom and a boron vacancy defect.

In many of other works, the single metal atoms were designed to be embedded in the surface at the sites of defects, or anchored above the dopant atoms of a 2D monolayer material. For example, the MoS_2 monolayer can act as a defect-free supporting material with a uniform distribution of anchoring sites for Pt single atoms (Du et al. 2015). It provides not only a very large surface-to-volume

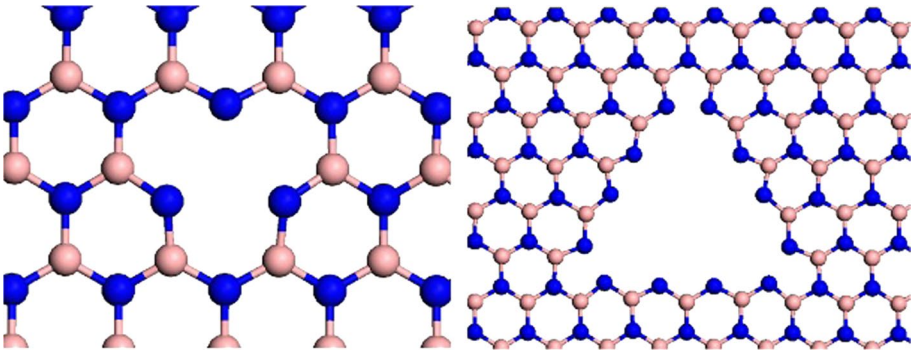

Fig. 7 Geometries (top view) of h-BNNS with the B vacancy (left) and N edge (right) defects. Color scheme: B, pink; N, dark blue. Adapted from Lin et al. (2013a, b)

ratio, but also a well-defined structure with a uniform distribution of anchoring points. $SrTiO_3$, the typical perovskite oxide, has attracted extensive interest in recent years. The Sr adatoms are well dispersed and have remarkably high thermal stability. They thus could serve as nucleation centers and guide the growth of an array of noble metal nanostructures. SAC $Ni_1/SrTiO_3$ was successfully prepared, which can be considered as a model system to investigate single-atom catalysis. Ti atoms can also be anchored on the Ti_2CO_2 monolayer, a typical MXene (Zhang et al. 2016a, b, c). The Ti_2CO_2 substrate could prevent Ti atoms from agglomerating. Ti/Ti_2CO_2 without any noble metal could exhibit very high activity for CO oxidation, which could be helpful to design more nonprecious metal nanocatalysts and shed light on MXene prospects as advanced materials. Single-layer, 2D periodic Fe-Pc through was synthesized by Abel and co-workers (Wang et al. 2015a, b, c). Unlike the graphene–metal system, such Fe-Pc sheet is an ideal material with single Fe atoms orderly and strongly anchored into the pores of the 2D polymeric Pc. The synthesis procedure is flexible so that Fe atoms can be replaced by other TM atoms. Inspired by the synthesis of Fe-Pc, Zhao et al. investigated systematically the catalytic behavior of TMs (Sc to Zn) combined in the context of polymeric Pc (Deng et al. 2013). The achievement provides a novel pathway to the long-standing dream of robust 2D atomic sheets with regularly and separately distributed 3d transition atoms for hydrogen storage and spintronics. In particular, it brings a new opportunity to realize a metal–substrate–catalyst for CO oxidation.

Other supports

Many other materials, including zeolites (Joseph et al. 2014), TiC (Sungeun et al. 2017), TiN (Sungeun et al. 2016), ion-exchange resin (Leilei et al. 2014), phosphomolybdic acid (PMA) (Zhang et al. 2016a, b, c), metal organic framework (MOF) (Zhang et al. 2016a, b, c), and others (Corma et al. 2015), were also used as substrates for the SACs.

PMA In coordination chemistry, catalytically active metal complexes in a zero- or low-valent state often adopt four-coordinate square planar or tetrahedral geometry. By applying this principle, Yan et al. developed a stable Pt_1 SAC on PMA-modified active carbon, which was achieved by anchoring Pt on the fourfold hollow sites on PMA (Fig. 8a) (Zhang et al. 2016a, b, c). Each Pt atom is stabilized by four oxygen atoms in a distorted square planar geometry, with Pt slightly protruding from the oxygen planar surface. Pt is positively charged, absorbs hydrogen easily, and exhibits excellent performance in the hydrogenation of nitrobenzene and cyclohexanone.

Zeolite Gates et al. reported the isolated gold atom supported in zeolite KLTL (Fig. 8b) (Joseph et al. 2014). The HAADF-STEM images indicate that single gold atoms appear as in the zeolite framework and only < 5% of the zeolite cages contained more than one gold atom. The atomic dispersion of the gold atoms is stabilized by the site isolation of the atoms in the zeolite. The appearance of an $Au–O_{zeolite}$ contribution indicated the formation of gold–support bonds. The results demonstrate a strong advantage of crystalline supports for fundamental understanding of supported catalysts.

TiC and TiN Lee et al. prepared a single-atom platinum catalyst on two different supports: titanium carbide (Pt_1/TiC) and titanium nitride (Pt_1/TiN) (Fig. 8c) (Sungeun et al. 2017). Pt_1/TiC showed higher activity, selectivity, and stability for electrochemical H_2O_2 production than Pt_1/TiN. DFT calculations presented that oxygen species have strong affinity into Pt_1/TiN, possibly acting as surface poisoning species, and Pt_1/TiC preserves oxygen–oxygen bonds more with higher selectivity toward H_2O_2 production. The work clearly shows that the support in SACs actively participates in the surface reaction and does not just act as anchoring sites for single atoms.

MOF MOFs, a class of porous and crystalline materials, provide the most effective coordination sites to anchor individual metal atoms, thereby preventing sintering during catalysis (Zhang et al. 2016a, b, c). The MOF can selectively capture and reduce carbon dioxide with

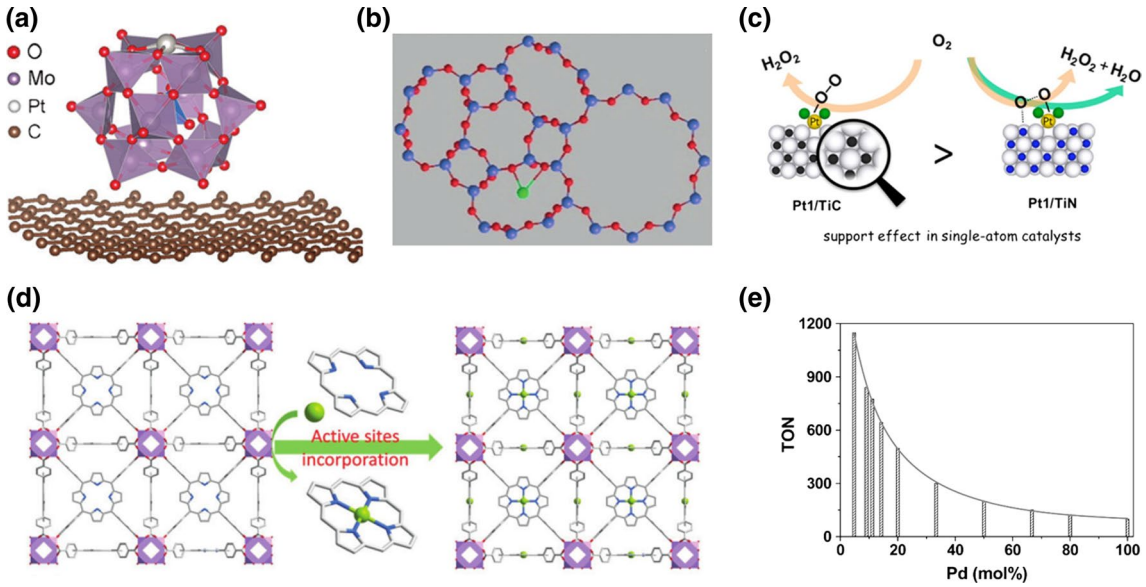

Fig. 8 **a** Side view of the most stable configuration of Pt_1 on PMA/graphene based on DFT calculations. **b** Models of zeolite KLTL with PtO_x located in the 8-membered ring at the C site. O is shown in red, T-site Si/Al in purple, Pt in green, N in blue, and H is not shown for clarity. **c** Schematic illustration of electrochemical H_2O_2 production by TiC- and TiN-supported Pt. **d** View of the 3D network of MOF-525-Co featuring a highly porous framework and incorporated active sites. **e** Turnover number (TON) values of Au/resin, Pd/resin, and a series of Au–Pd/resin for the Ullmann reaction of chlorobenzene. Adapted from Joseph et al. (2014), Leilei et al. (2014), Sungeun et al. (2017) and Zhang et al. (2016a, b, c)

high efficiency under visible light irradiation. Mechanistic investigation indicates that the presence of single Co atoms in the MOF can greatly boost the electron–hole separation efficiency in porphyrin units (Fig. 8d). Directional migration of photogenerated excitons from porphyrin to catalytic Co centers was witnessed, then achieving supply of long-lived electrons for the reduction of carbon dioxide molecules adsorbed on the Co centers. As a direct result, porphyrin MOF comprising atomically dispersed catalytic centers shows significantly enhanced photocatalytic conversion of carbon dioxide.

Ion-exchange resin Zhang et al. reported the single-atom catalysts Au_1/resin, Pd_1/resin, and a series of Au–Pd/resin, which could serve as an effective and robust catalyst for the Ullmann reaction of aryl chlorides in aqueous media (Fig. 8e) (Leilei et al. 2014). The catalyst showed high activity and excellent stability with broad substrate scope and functional group tolerance. The high atom efficiency, combined with the unique geometrical structure and the electronic properties of the special active site entities, made the resin-supported Au and Pd single atoms unique catalysts for aryl chloride activation. Diffuse reflection infrared Fourier transform (DRIFT) spectra showed that the resin support may impose an electronic effect on the Au and Pd atoms thereon.

Preparation methods

A prerequisite for the application of SACs is to prepare highly dispersed single atoms of a defined species on appropriate supports. Fabrication of SACs, however, has been challenging because of the tendency toward aggregation of single metal atoms either during the synthetic processes or the subsequent treatments. We will discuss below a few methods that have been utilized to prepare SACs.

The mass-selected soft-landing technique

The mass-selected soft-landing method has proved to be extremely powerful for synthesizing metal clusters with a precisely controlled number of atoms (Lei et al. 2010; Abbet et al. 2000; Kaden et al. 2009) and it can also be used to prepare SACs. It can provide excellent model catalysts for fundamental studies of metal–support interactions on the atomic level. Many experimental and theoretical studies based on this method have addressed the catalytic properties of metal species on supports (Abbet et al. 2000; Heiz et al.1999; Ja et al. 2009). For example, Abbet et al. prepared the size-selected Pd_n clusters ($1 < n < 30$) supported on thin MgO (100) films by this method and studied the cyclotrimerization of acetylene by thermal desorption and diffuse reflectance infrared Fourier transform spectroscopy (DRIFTS).

Surprisingly, the production of benzene was observed on a single palladium atom at low temperature (300 K). Using DFT calculations, they show that free inert Pd atoms were activated by charge transfer from defect sites of the MgO substrate upon deposition. However, such an expensive and low-yield fabrication method limits its wide application and is clearly not suitable for practical industrial applications of heterogeneous catalysis.

Atomic layer deposition (ALD)

The ALD technique is powerful since the technique can provide desired model catalysts for studying fundamental mechanisms of catalytic processes and the effects of particle size, nature of the support surfaces, overlayers on metal or alloy nanoparticles, and so on. ALD allows one to control the size, morphology, density as well as the loading of the deposited metal. Sun et al. (2013) employ the ALD technique to fabricate single-atom Pt on the surfaces of grapheme nanosheet supports. The Pt loading on graphene was accurately controlled by the number of ALD cycles. The catalytic activity of the Pt/grapheme was significantly improved, which is one order of magnitude higher than that of the commercial Pt/C catalyst. Lei et al. synthesized thin film-stabilized single Pd atom using ALD (Piernavieja-Hermida et al. 2016). The thermal stability of the supported Pd SAC is significantly enhanced by creating a nanocavity thin film structure. The single Pd atom was anchored on the surface by chlorine sites. The thin film-stabilized Pd SAC was thermally stable under both oxidation and reduction conditions. The catalytic performance in the methanol decomposition reaction is found to depend on the thickness of protecting layers. These results clearly show that the ALD nanocavities provide a basis for future design of SACs that are highly efficient and stable. As a method for preparing better-controlled nanocluster catalysts for fundamental study, it is expected that ALD can become a powerful tool for studying the synthesis–structure–performance relationships of supported metal catalysts including supported metal SACs.

Wet chemistry methods

The wet chemistry approach does not require specialized equipment and can be routinely practiced in any wet chemistry laboratory. Therefore, it is the preferred method for commercial production of supported metal catalysts. In this method, the precursor materials already contain single-atom metal species, and the objective is to anchor the metal complexes onto the supports through a chemical reaction while avoiding their aggregation during the synthesis and post-treatment processes. So far, SACs have been synthesized mainly by wet chemical routes.

Co-precipitation By the nature of the co-precipitation process, a uniform distribution of the different active species can be obtained on a molecular level. The characteristics of the final catalysts, however, depend on many parameters, such as the order and the speed of the addition of the component solutions, the sizes of the droplets, efficient mixing, the temperature of the base solution, the pH value, and the aging time. Supported noble metal SACs have been synthesized by co-precipitation (Qiao et al. 2011, 2015a, b; Lin et al. 2012, 2013a, b, 2015; Wei et al. 2014; Liang et al. 2014; Kuo et al. 2012). For example, Zhang and co-workers reported the synthesis of the single-atom catalyst Pt_1/FeO_x by co-precipitation of an aqueous solution of chloroplatinic acid with sodium carbonate at 50 °C, with the pH value of the resulting solution controlled at about 8 (Qiao et al. 2011). The single-atom catalyst showed excellent stability and high activity for both CO oxidation and preferential oxidation. They also prepared the $Ir_1/FeOx$ catalyst with an Ir loading of merely 0.01 wt% by an improved co-precipitation method (Lin et al. 2013a, b). Supported Ir catalysts were found to exhibit excellent performances in reactions, such as CO oxidation, hydrogenation, and dehydrogenation. A major issue for this approach to synthesizing metal SACs is that some metal atoms can be buried at the interfacial regions of the support agglomerates and within the bulk of the support crystallites. These buried single atoms are thus not accessible by the reactant molecules, significantly compromising the effectiveness and efficiency of the SACs.

Impregnation The impregnation method is suitable for preparing SACs on open supports. The process depends on the capability of the support surface to adsorb the precursor complexes. The final amount of metal loading and dispersion strongly depends on the nature of the anchoring sites on the support surfaces. By controlling the types of metal precursors and their interactions with the support anchoring sites, localization of the desired single metal atoms can be primarily controlled. Gates and co-workers made the isolated gold atom on zeolite NaY by impregnating the $Au(CH_3)_2$ into the calcined zeolite in a Schlenk flask, which was slurried in dried *n*-pentane at 298 K for 24 h (Lu et al. 2012). They also prepared the single-atom platinum supported on Zeolite KLTL by this method (Joseph et al. 2014). Xiong et al. used this method to produce stable Pt_1/CeO_2 SAC (Benjamin et al. 2016). The SAC was tested for CO oxidation and demonstrated sintering-resistant behavior at high temperatures. Narula et al. reported the single Pt atoms supported on θ-Al_2O_3 (010) surface by this method (Melanie et al. 2013). The obtained single-atom catalyst Pt/θ-Al_2O_3 exhibited high activation ability to the CO oxidation and NO oxidation (Narula et al. 2014).

Deposition–precipitation This method is extremely powerful for producing uniformly distributed single metal atoms with very low levels of metal loading, which involves the precipitation of a metal hydroxide or carbonate on the supports via the reaction of a base with metal salt complexes. For example, Liu et al. reported the CeO_2-supported Au single atoms (Au_1/CeO_2), which was highly active, selective, and extremely stable for preferential oxidation of CO (Botao et al. 2015). Zhang et al. prepared the SAC Au_1/Co_3O_4 (Qiao et al. 2015a, b). The obtained catalyst exhibited extremely high activity for CO oxidation. Xiang-Kui et al. (2014) synthesized the Au_1/ZnO and Pt_1/ZnO SAC. The isolated precious metal atoms including Pt_1 and Au_1 together with coordinated lattice oxygen embedded onto ZnO surfaces provide single, yet stable, active sites for methanol steam reforming.

Other methods

Ion implantation When 2D materials such as oxide sheets, graphene, and dichalcogenides are used as support materials, the low-energy ion implantation method can be used to produce highly doped materials. Such a method can be adapted to fabricate model metal or even nonmetal SACs for investigating the catalytic behavior of highly doped 2D catalytic materials. Telychko et al. reported a straightforward method to produce high-quality nitrogen-doped graphene on SiC (0001) using direct nitrogen ion implantation and subsequent stabilization at temperatures above 1300 K (Mykola et al. 2014). They demonstrated that double defects, which comprise two nitrogen defects in a second-nearest-neighbor configuration, can be formed in a controlled way by adjusting the duration of bombardment.

Pyrolysis synthesis This method is generally used for preparing carbon-based catalysts. High-metal-loading SACs can also be produced via this method with high-surface-area carbon supports. N-doped porous carbons are usually the preferred choice of supports. For instance, Fei et al. (2015) reported an electrocatalyst for hydrogen generation based on very small amounts of cobalt dispersed as individual atoms on nitrogen-doped graphene. This catalyst was robust and highly active in aqueous media with very low overpotentials (30 mV). A variety of analytical techniques and electrochemical measurements suggest that the catalytically active sites are associated with the metal centers coordinated to nitrogen.

High-temperature vapor transport This method has recently been used to produce thermally stable Pt_1/CeO_2 SAC (John et al. 2016). At high temperatures and under oxidizing conditions, Pt can be emitted as volatile PtO_2 molecules. The PtO_2 molecules are captured by the surfaces of CeO_2 support which stabilize the PtO_2 molecules; then, single Pt atoms can be uniformly dispersed onto the CeO_2 surface. The SAC was tested for CO oxidation and demonstrated sintering-resistant behavior at high temperatures. This technique may be applicable to synthesizing other types of stable SACs.

Anti-Ostwald ripening Tang et al. obtained a stable supported Ag SAC with a controllable electronic state by anti-Ostwald ripening (Zhiwei et al. 2012; Pingping et al. 2014). The Ag atoms were initially dispersed and then thermally migrated along the external surfaces to the ends of the hollandite-type manganese oxide nanorods, and were consecutively inserted in the tunnels of the hollandite-type manganese oxide to form single-atom Ag chains, resulting in single Ag atoms anchored at the tunnel openings of the HMO. The Ag SAC exhibited high activation ability to both lattice oxygen and molecule oxygen, which resulted in excellent activity in oxidizing HCHO at low temperatures.

Characterizations of SACs

Confirming the existence of only isolated single metal atoms and determining their spatial distribution are critical to developing SACs. Recent advances in characterization techniques with atomic resolution, as well as DFT calculations, can provide information about the dispersion of single atoms on supports and deep insights into understanding the stability of and catalysis by supported single metal atoms.

Scanning transmission electron microscopy (STEM)

STEM is the most convincing and intuitive approach to confirm the existence of isolated single metal atoms, which can directly image the single metal atoms, identify their location, and determine the spatial distribution (Guang et al. 2015; Melanie et al. 2013; Zhang et al. 2014). Figure 9 shows the HAADF-STEM images of a series of Ir/FeO_x catalysts (Lin et al. 2013a, b). The individual Ir atoms (bright dots, labeled with white circles) are clearly visible with excellent image contrast. It also reveals that the individual Ir atoms occupy exactly the positions of the Fe atoms. Such a technique is indispensable to developing and optimizing synthetic methods that reliably produce metal SACs. The application of STEM in the past few years has provided invaluable information on the nature of supported metal SACs and in optimizing synthesis protocols to fabricate supported metal SACs (Chunlei et al. 2017; Qiao et al. 2015a, b; Flytzani-stephanopoulos 2014).

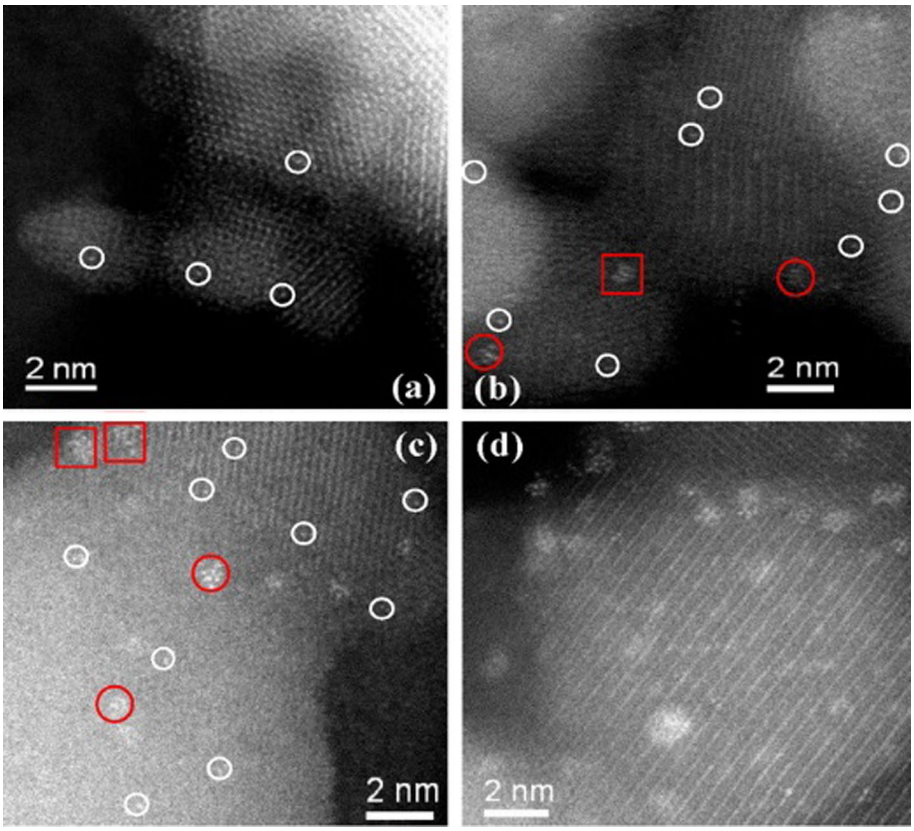

Fig. 9 HAADF-STEM images and the frequencies of the observed size scope of Ir/FeO_x with the Ir loadings from 0.01 to 2.40 wt%. **a** Ir_1/FeO_x; **b** Ir/FeO_x-0.22; **c** Ir/FeO_x-0.32; **d** Ir/FeO_x-2.40. Adapted from Lin et al. (2013a, b)

EXAFS

The EXAFS technique has been extensively used to characterize the nature of supported metal nanoparticles or clusters (Alexeev and Gates 2000; Greecor and Lytle 1980; Gates 1995; Thomas et al. 2005; Ogino 2017). The EXAFS can also be effectively utilized to evaluate the fabrication by determining the metal–metal coordination numbers. For example, it was successfully applied to evaluating the nature of Pt_1/FeO_x catalysts (Wei et al. 2014). As clearly shown in Table 2, for the catalyst 0.08% Pt/FeO_x-R200, there were a Pt–O contribution at 2.01Å with a coordination number of 3.9 and a Pt–Fe contribution at 3.05Å with a coordination number of 3.3. The much longer distance of Pt–Fe coordination (3.05 Å) than that in Pt–Fe alloy (2.54Å) suggests that Pt does not directly coordinate with Fe. Instead, it coordinates with Fe via bridging O. The relatively higher coordination number of Pt–O (3.9) also supports this conclusion. Of most importance, there was no direct Pt–Pt coordination in this catalyst, suggesting that the Pt existed exclusively as isolated single atoms. When the reduction temperature was increased to 250 °C (0.08% Pt/FeO_x-R250), the EXAFS data did show the formation of Pt–Pt bonding but with a distance much longer than that of Pt–Pt distance in bulk Pt. This suggests that a certain degree of aggregation of Pt atoms occurred during the 250 °C reduction treatment. With further increase in Pt loading to 0.75, 2.73, and 4.30 wt% while retaining the reduction temperature of 250 °C, the Pt–O coordination decreased, while the Pt–Pt metallic bonding started to occur and then steadily increased. The Pt–Pt coordination number, however, was relatively low (0.5–2.3) for the above three catalysts, indicative of the formation of very small Pt clusters or particles.

XANES

The XANES can provide information about the dispersion of single atoms, the nature of the neighboring atomic species, and their oxidation states. Figure 10 shows the normalized XANES spectra on the set of Pt_1/FeO_x catalysts (Wei et al. 2014). The white-line intensity, reflecting the oxidation state of the Pt species, increased steadily with a decrease in the Pt loading, which suggests that the Pt became more positively charged with lower Pt loading. In other words, lower Pt loading results in higher percentage of single-atom and pseudo-single-atom structures in the catalyst, and more electrons transfer from Pt to the FeO_x support. Moreover, with the same Pt loading of 0.08 wt%, the 250 °C reduction treatment resulted in lower white-line intensity than that of the catalyst with a 200 °C reduction treatment. The changing pattern for the white-line intensity is consistent with that of

Table 2 EXAFS date fitting results of Pt/FeO_x with different Pt loading. Adapted from Wei et al. (2014)

Sample	Shell	*N*	*R*(Å)	$\sigma^2 * 10^2$ (Å^2)	ΔE_0 (eV)	r-factor (%)
Pt foil	Pt–Pt	12.0	2.76	0.41	6.1	0.42
PtO_2	Pt–O	6.0	2.00	0.41	7.2	0.56
	Pt–Pt	6.0	3.08	0.99	2.1	
4.30% Pt/FeO_x-R250	Pt–O	0.6	1.95	0.30	− 3.5	0.77
	Pt–Fe	1.5	2.52	0.82	− 3.5	
	Pt–Pt	2.3	2.62	0.82	− 3.5	
2.73% Pt/FeO_x-R250	Pt–O	1.4	2.00	0.30	6.4	0.95
	Pt–Fe	0.8	2.54	0.54	6.4	
	Pt–Pt	1.4	2.68	0.54	6.4	
0.75% Pt/FeO_x-R250	Pt–O	1.8	2.00	0.17	5.1	1.14
	Pt–Fe	0.9	2.52	0.36	5.1	
	Pt–Pt	0.5	2.73	0.36	5.1	
0.08% Pt/FeO_x-R250	Pt–O	2.0	2.01	0.26	8.4	0.13
	Pt–Fe	1.0	2.55	0.47	8.4	
	Pt–Pt_{long}	1.1	2.99	0.47	8.4	
0.08% Pt/FeO_x-R200	Pt–Fe_{long}	0.8	3.08	0.47	8.4	0.27
	Pt–O	3.9	2.01	0.11	7.4	
	Pt–Fe_{long}	3.3	3.05	1.09	7.4	

N, the coordination number for the absorber–backscatterer pair; *R*, the average absorber–backscatterer distance; σ^2, the Debye–Waller factor; ΔE_0, the inner potential correction. The accuracies of the above parameters were estimated as N, ± 20%; R, ± 1%; δ^2, ± 20%; ΔE_0, ± 20%. The data ranges used for data fitting in k-space (Δk) and R-space (ΔR) are 3.0-10.7Å^{-1} and 1.2-3.5Å, respectively

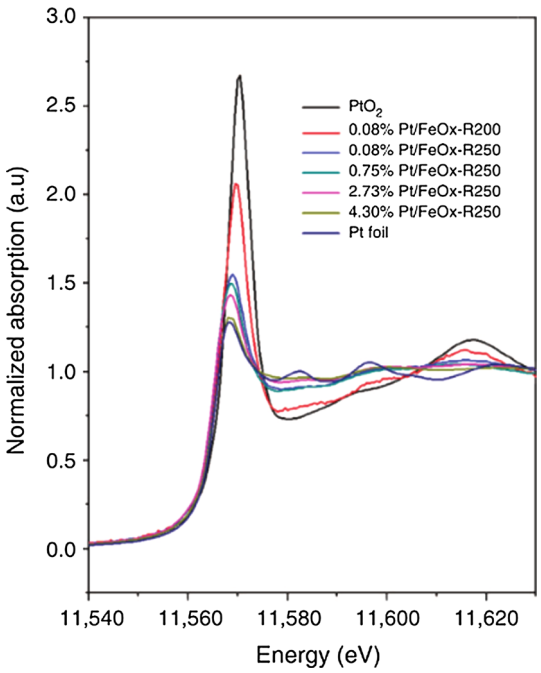

Fig. 10 Normalized XANES spectra at Pt L_{III}-edge of different Pt_1/FeO_x samples. Adapted from Wei et al. (2014)

the Pt–O coordination number, providing further evidence that the electronic property of Pt can be effectively tuned by forming unique nanoscale or atomic-scale Pt structures.

Infrared spectroscopy (IR)

With appropriate probe molecules, IR can be used to evaluate the existence of single metal atoms and to quantify the percentage of the dispersed single metal atoms (Matthew and Phillip 2016; Chithra et al. 2017). The advantages of the IR technique include quantification and in situ monitoring during a catalytic reaction. The combination of this technique with HAADF-STEM, EXAFS, and XANES provides a powerful tool box for studying SACs. Stair et al. showed that IR spectroscopy with CO as a probe molecule can differentiate and quantify both Pt single atoms and nanoparticles (Kunlun et al. 2015). Recently, DRIFTS with known site-specific extinction coefficients was used to quantify the fraction of isolated single-atom Rh sites in supported Rh catalysts that consist of mixtures of Rh single atoms and nanoparticles (Lang et al. 2016). As shown in Fig. 11, for the 0.03% Rh_1/ZnO, two obvious peaks at 2087 and 2014 cm^{-1} are assigned to the symmetric and asymmetric vibration of *gem*-dicarbonyl doublet CO on positively charged Rh atoms, respectively, and another peak at 2060 cm^{-1} is attributed to the linear CO on the Rh^0 atom. The absence of bridged CO indicates that Rh atoms are singly dispersed on the ZnO support. Studies showed that if the position of IR peaks remains the same under decreased CO coverage, these peaks could probably be attributed to CO adsorbed on a single metal atom (Cavanagh and Yates 1981). Therefore, lack of a shift

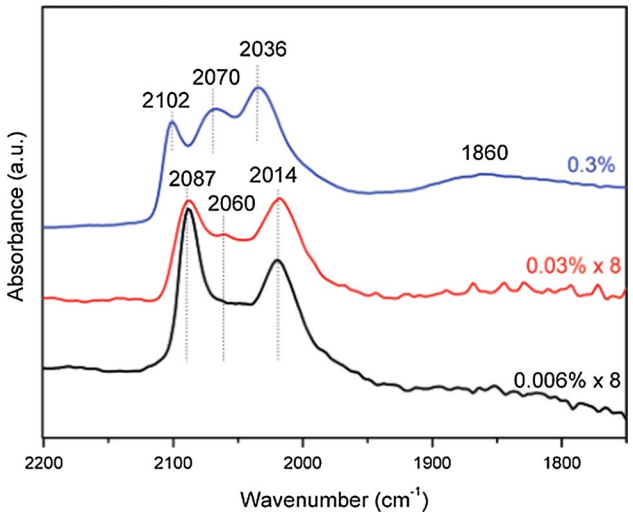

Fig. 11 DRIFT spectra of CO adsorption at 258 °C on Rh_1/ZnO catalysts with different Rh loadings. All spectra were collected after CO adsorption (10 min) and He purging (10 min). Adapted from Lang et al. (2016)

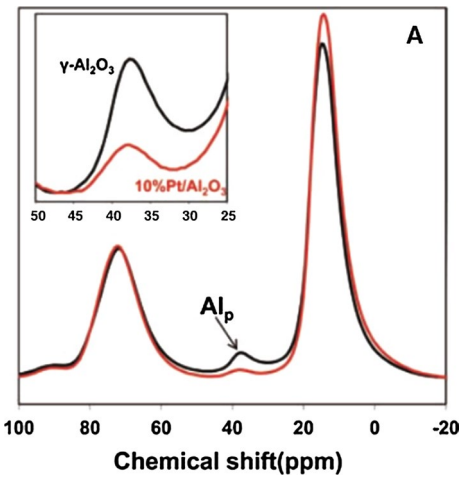

Fig. 12 ^{27}Al MAS-NMR spectra of γ-Al_2O_3 (black) and 10 wt% Pt_1/γ-Al_2O_3 (red). Adapted from Ja et al. (2009)

for the linear Rh^0-CO at 2060 cm^{-1} further proves that Rh atoms are primarily isolated from each other on the support.

Nuclear magnetic resonance spectroscopy (NMR)

Solid-state magic angle spinning NMR (MAS-NMR) can provide information about the nature of metal species and binding ligands during a catalytic reaction (Zhang et al. 2012a, b). This technique has been effectively utilized to study the anchoring of single Pt atoms on γ-Al_2O_3 supports (Ja et al. 2009). As shown in Fig. 12, the spectrum of the metal-free oxide support exhibits three peaks centered at 13, 35, and 70 parts per million (ppm) chemical shifts. The two characteristic ^{27}Al NMR features of γ-Al_2O_3 at 13 and 70 ppm represent Al^{3+} ions in octahedral (Al^{3+}_{octa}) and tetrahedral (Al^{3+}_{tetra}) coordination, respectively. The NMR peak at 35 ppm chemical shift has been assigned to Al^{3+} ions in pentahedral coordination (Al^{3+}_{penta}). Loading Pt onto the γ-Al_2O_3 support and calcining the catalyst material at 573 K results in a substantial decrease in the number of Al^{3+}_{penta} sites, as evidenced by the large drop in the intensity of the 35-ppm NMR peak. Concomitantly, the intensity of the 13-ppm NMR feature increases with the loading of Pt onto γ-Al_2O_3, which suggests the conversion of the Al^{3+}_{penta} sites into Al^{3+}_{octa}. These results strongly suggest that Pt atoms bind to the Al^{3+}_{penta} sites on the γ-Al_2O_3 surface through oxygen bridges, thereby coordinatively saturating these sites.

Theoretical calculations

The theoretical DFT calculations have proved to be extremely important for understanding the fundamental mechanisms of catalysis by supported SACs (Yan et al. 2017a, b). The combined use of theoretical DFT calculations with advanced characterization techniques has provided deep insights into understanding the stability of and catalysis by supported single metal atoms. For example, Neitzel et al. (2016) investigated the stability and the reactivity of M_1

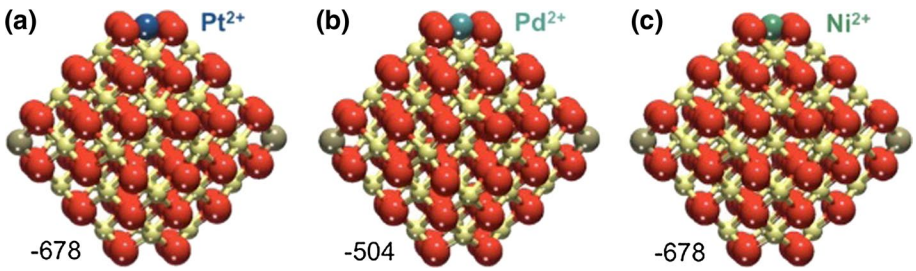

Fig. 13 Adsorption energies (kJ/mol) of **a** Pt^{2+}, **b** Pd^{2+}, and **c** Ni^{2+} species (with respect to free neutral atoms) in square planar coordination on the $Ce_{40}O_{80}$ nanoparticles. Yellow, brown, and red spheres represent Ce^{4+} cations, Ce^{3+} cations, and O^{2-} anions, respectively. Adapted from Neitzel et al. (2016)

(M = Pt, Pd, and Ni) species on nanostructured CeO_2 films by DFT calculations and spectroscopy techniques (Fig. 13). They found that all the M_1^{2+} species possess higher adsorption energies than their corresponding cohesive energies in the bulk metals. While both the Pt^{2+} and Pd^{2+} species can activate H_2, the Ni–CeO_2 system does not exhibit such reactivity due to the extremely strong binding of the Ni^{2+} species. Aleksandrov et al. (2015) employed DFT calculations to predict the structure and relative stability of Pt atom on $Ce_{21}O_{42}$. The DFT calculations indicated that Pt^{2+} is the most stable Pt species, which coordinated in a square planar complex with four oxygen anions as ligands on small CeO_2 facets. Even under partial reduction conditions, the Pt^{2+} species were still stable. When the Pt species were located on other positions, they maintain the metallic nature and may not be stable. The use of DFT calculations should help to understand the experimentally observed phenomena and to help design better SACs.

Properties of SACs

Location and strong metal–support interactions (SMSIs)

The locations of single atoms are correlated with the anchor sites of the support. It was found that very low levels of metal loading noble metal atoms can substitutionally dope the various types of metal oxides. The substitutionally doped metal atoms may carry a positive charge and thus influence their binding strengths for reactant molecules or modulate their behavior. By using a combination of photoelectron spectroscopy, it was concluded that Pt single atoms on ceria are stabilized by the monatomic step edges. Pt segregation at steps leads to stable dispersions of single Pt^{2+} ions in planar PtO_4 moieties, which incorporate excess oxygen atoms and thus contribute to oxygen storage capacity of ceria (Dvořák et al. 2016). By utilizing a 2D titania layer with periodic 6- and 10-membered nanopores of a reconstructed $SrTiO_3$ (110) surface as substrate, Wang et al. (2014a, b) anchored Ni single adatoms onto the open pores and found that an in-gap state induced an upward band bending. By employing a photochemical approach to fabricating stable supported SACs, Liu et al. dispersed Pd single atoms on ethylene glycolate-stabilized ultrathin TiO_2 nanosheets (Pengxin et al. 2016). Yang et al. demonstrated that Na and K can stabilize Au single atoms along with hydroxyl and oxo groups. They have used UV-assisted methods to prepare mononuclear Au-$O(OH)_x$ species onto titania with a loading level up to 1.2 wt% (Ming et al. 2014). The anchoring and localization of single metal atoms on high surface area supports will enable the practical applications of supported metal SACs. Different types of surface atoms and surface cation or anion vacancies interact with the single metal atoms differently via various types of synthesis approaches.

The support plays a crucial role in the chemical activity and selectivity of the deposited nanocatalysts, as first recognized by Tauster et al. (1978) known as the SMSI in 1978. SMSIs arising from interfacial bonding are crucial to the understanding of SAC, and this not only determines whether guest metal atoms in SACs can be tightly anchored onto the support, but also plays a significant role on the subsequent catalysis. According to the nature of the interaction, SMSIs can be mainly divided into two types: one stemming from electronic defects and the other one mainly caused by surface structural defects. SMSIs of electronic defects have been proved to be capable of anchoring individual atoms tightly, either through direct M_2–M_1 bonding or through the formation of M_2–O–M_1, in which M_1 and M_2 represent the supported metal atom and the metal cation of the support, respectively. The second type of SMSI, namely structural defects, can be surface steps, coordinatively unsaturated sites, surface vacancies, or other types of surface defects. Owing to the advantage of multiple bonding with more than one adjacent oxygen atom, some vacancies on specific supports have been found to be superior anchoring sites for single atoms, such as the aluminum vacancies of g-Al_2O_3 and the iron vacancies on Fe_2O_3 for Pt atoms, and the zinc vacancies of ZnO for Au atoms.

Geometric and electronic effects

Supported SACs possess unique geometric and electronic properties caused by the special locations of single atoms and SMSIs. A straightforward geometric effect of single atoms is that SACs make full use of all active metal atoms, which is the primary motivation for reducing metal size to atomic level. Another geometric effect of the SACs is homogenized active sites, which are all well defined and atomically distributed on the supports, resulting in an identical geometric structure of each active center, similar to that of a homogeneous catalyst. Meanwhile, since only single-atom metal active sites are available in SACs, different catalytic mechanism might take place. For example, contiguously located Pd sites function as the active sites for the elementary step of N_2O decomposition, while the rate-determining step was found to have been changed by forming Pd single atoms on a Au surface (Wei et al. 2012). Supported single atoms are usually more reactive due to their unsaturated coordination environment. Their electronic structures are much more volatile due to their coordinated environments. The bonding of single atoms with the uncapped sites on the supports leads to charge transfer between single atoms and the support owing to different chemical potentials. As a result, the anchored single atoms usually carry some charge, which was verified by various spectral measurements and

computational modeling (Simon et al. 2007; Kwang et al. 2009; Zhang et al. 2005; Shapovalov and Metiu 2007; Song et al. 2013). On the other hand, the conjunction of single metal atom with the surface groups of supports also leads to the bonding or coupling of quantum levels of single metal atoms with surface species. Taking Pt_1/FeO_x as an example (Qiao et al. 2011), the calculated Bader charges show that Pt atoms are positively charged when anchored on FeO_x and it was found that the discrete 5*d*-orbitals of Pt atom are mixed considerably with the O_{2p} band and evolved to *d*-band.

Applications of SACS

Supported noble metal nanoparticles and nanoclusters are among the most important catalysts that enable many critical technologies, for example, environmental remediation and energy production (Wang et al. 2015a, b, c; Jia and Wang 2015; Liu et al. 2014; Zhou et al. 2017). In recent years, SACs have also demonstrated notable catalytic performances in various reactions, such as oxidation reactions, hydrogenation reactions, dehydrogenation reactions, water–gas shift reaction, reforming reactions, as well as electrocatalysis and photocatalysis reactions. In many cases, SACs are catalytically active and can be extremely stable during catalytic reactions. Below, some representative research, as well as the advances of single-atom catalysis, is summarized.

Oxidation reactions

SACs have demonstrated great potential in a variety of oxidation reactions, including CO (Kunlun et al. 2015; Qiao et al. 2011; Mao et al. 2014; Melanie et al. 2013; Liang et al. 2014; Long et al. 2016; Lin et al. 2013a, b; Song et al. 2013; Li et al. 2014), preferential oxidation of CO (Kuo et al. 2012; Qiao et al. 2015a, b) HCHO (Zhiwei et al. 2012; Pingping et al. 2014), NO (Narula et al. 2014), glucose (Zhang et al. 2014), methanol (Sun et al. 2013), ethanol(Songhai et al. 2012), methane(Guo et al. 2014), and formic acid (Sungeun et al. 2016; Sungeun and Hyunjoo 2013). In the following, we will discuss a few selected examples to illustrate the broad applications of supported single metal atoms for oxidation reactions.

CO oxidation

Low-temperature CO oxidation is of both fundamental and practical importance in catalytic chemistry due to the impending demand of environmental protection and the removal of CO contaminations from H_2-rich fuel gases for polymer electrolyte fuel cells among many other industrial processes. SAC of Pt_1/FeO_x could provide isolated and positively charged Pt atoms, in turn capable of largely lowering the CO adsorption energy (Qiao et al. 2011). This SAC exhibited excellent stability and high activity for both CO oxidation and preferential oxidation. Possible pathways of the CO oxidation were proposed, as shown in Fig. 14. After pre-reduction by H_2, the stoichiometric hematite surfaces near the Pt atoms are reduced partially to an oxygen vacancy (step i), which can adsorb O_2. In this case, the oxygen coordination number of Pt changes from three to two. The adsorbed oxygen ($O_{2,ad}$) is well activated on Pt single atoms (step ii). The binding energy of the adsorption of CO on the single Pt atoms is 1.27 eV

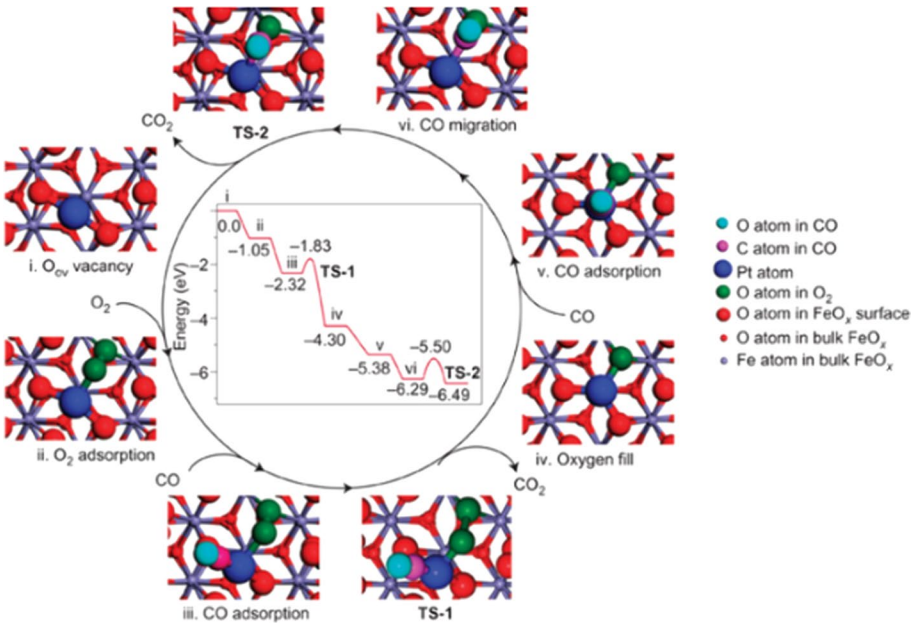

Fig. 14 Proposed reaction pathways for CO oxidation on the Pt_1/FeO_x catalyst. Adapted from Qiao et al. (2011)

(step iii). The calculated activation barrier for reaction of $CO_{ad} + O–O_{ad} \rightarrow CO_2 + O_{ad}$ (TS-1) is 0.49 eV. After the release of the CO_2, the surface oxygen vacancy is healed by the remaining O_{ad} atom, which restores the Pt-substituted stoichiometric hematite surfaces (step iv). When the second CO molecule is adsorbed on Pt (step v), a new reaction of $CO_{ad} + O–O_{ad} \rightarrow CO_2 + O_{vac}$ occurs (step vi and TS-2). The calculated barrier of this reaction is 0.79 eV. After releasing the second CO_2, the Pt-embedded stoichiometric surface is reduced again to form a new oxygen vacancy (step i). This multistep procedure thus finishes the catalytic cycle. The two CO oxidation reactions of $CO_{ad} + O–O_{ad}$ and $CO_{ad} + O_{ad}$ both follow Langmuir–Hinshelwood mechanisms.

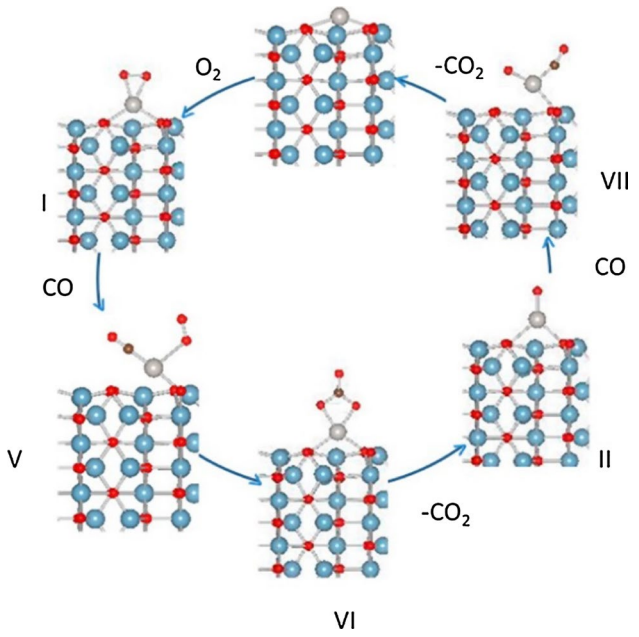

Fig. 15 Pathway for CO oxidation on single Pt atoms supported on the (010) surface of θ-Al_2O_3 (oxygen: red, aluminum: light blue, platinum: light gray, and carbon: brownness). Adapted from Melanie et al. (2013)

Narula and co-workers studied CO oxidation on single Pt atoms supported on θ-Al_2O_3 and proposed different pathway based on their experimental results and theoretical calculations (Melanie et al. 2013). First of all, the supported Pt single-atom preferred to bond to O_2 rather than CO. Then, CO bonded with the oxygenated Pt atom and formed a carbonate then dissociates to liberate CO_2, leaving an oxygen atom on Pt. Finally, the catalyst was regenerated through subsequent reaction with another CO molecule, as shown in Fig. 15. The pathway proposed was convincing because strong evidence of CO_3 coverage that ought to occur was found. The proposed mechanism of CO oxidation is very different from that on Pt_1/FeO_x where the oxygen vacancies on the support surface play an important role.

Li et al. investigated CO oxidation catalyzed by single Au atoms supported on thoria (Au/ThO_2) (Long et al. 2016). The results revealed a new mechanism of CO oxidation on a gold adatom supported by ThO_2 (111), where O_2 is adsorbed only at the Th site on the surface, and the gas-phase CO then reacts directly with the activated O_2* to form CO_2, which is the rate-limiting step, with a barrier of 0.46 eV (Fig. 16). It was found that CO oxidation can occur without CO and O_2 co-adsorption on Au, which was previously considered a key intermediate. The results provide new insights into CO oxidation on isolated gold atoms supported by the 5f-element compound ThO_2 (111). This mechanism can help clarify the catalytic cycle of CO oxidation, support the design of high-performance low-cost catalysts, and elucidate the redox properties of actinide oxides.

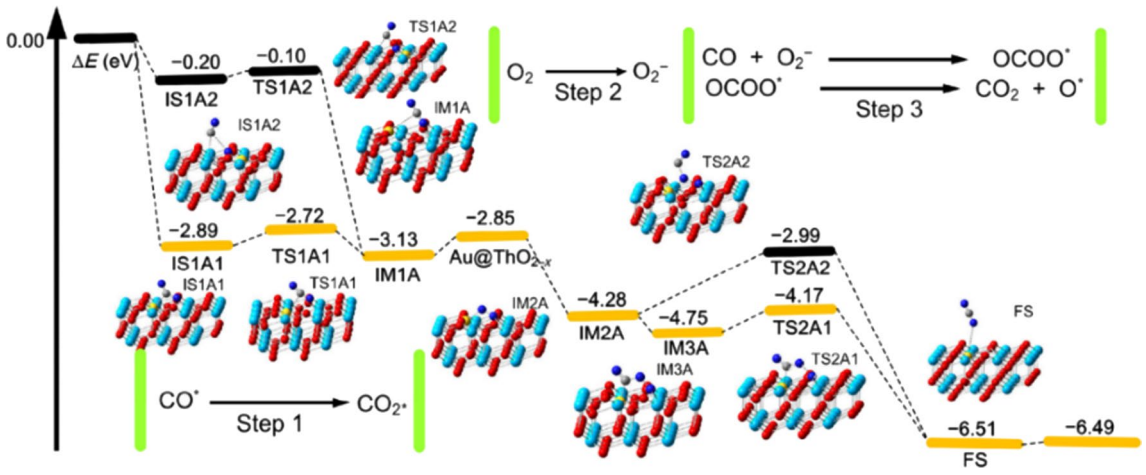

Fig. 16 Calculated potential energy profile of CO oxidation on Au-doped ThO_2 (111) (oxygen of ThO_2: red, thorium: light blue, gold: yellow, carbon: light gray, and adsorbed oxygen: blue). Adapted from Long et al. (2016)

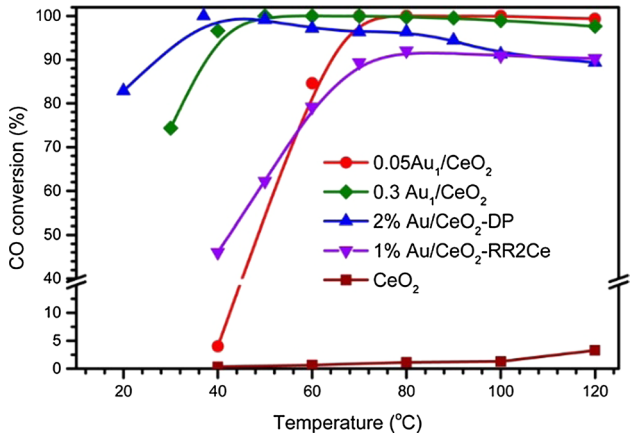

Fig. 17 CO conversion as a function of reaction temperature for PROX on Au/CeO_2. Reaction condition: 1 vol% CO + 1 vol% O_2 + 40 vol% H_2 balanced with He. Adapted from Qiao et al. (2015a, b)

Preferential oxidation of CO

Preferential oxidation of CO (PROX) in H_2-rich stream is critical to the production of clean H_2 for the H_2-based fuel cells, which provide clean and efficient energy conversion. Development of highly active and selective PROX catalysts is very desirable but proved to be extremely challenging. As shown in Fig. 17, Qiao et al. (2015a, b) reported that CeO_2-supported Au single atoms (Au_1/CeO_2) are highly active, selective, and extremely stable for PROX with > 99.5% CO conversion over a wide temperature range, including the working temperature of proton exchange membrane fuel cells. The high CO conversion realized at high temperatures is attributed SAC's unique property of being unable to dissociatively adsorb H_2 and thus has a low reactivity toward H_2 oxidation. As Au clusters or nanoparticles significantly oxidize H_2 at temperatures > 80 °C, they are not fit for PROX reactions with high temperature. This strategy was proved in general and can be extended to other oxide-supported Au atoms (e.g., Au_1/FeO_x), which may open a new window for the efficient catalysis of the PROX reaction.

NO oxidation

Oxides of nitrogen (NO_x) are highly reactive gases that are emitted from cars, trucks, and buses, power plants, and off-road equipment. These oxides are known to have adverse effects on the human respiratory system. The abatement of nitrogen oxides generally involves an oxidation step to convert them all to NO_2 which can then be reduced to nitrogen. NO oxidation on supported Pt single atoms has been studied (Narula et al. 2014). The first-principles DFT modeling suggested that NO oxidation is feasible on fully oxidized single θ-Al_2O_3-supported Pt atoms via a modified Langmuir–Hinshelwood pathway, which is in contrast to the known decrease in NO oxidation activity of supported Pt with decreasing Pt particle size believed to be due to increased Pt oxidation. Experimental data indicate that remarkable NO oxidation activity was obtained by the θ-Al_2O_3-supported Pt single atoms (Fig. 18). A comparison of turnover frequencies of single supported Pt atoms with those of Pt particles for NO oxidation shows that single supported Pt atoms are as active as fully formed platinum particles. The overall picture of NO oxidation on supported Pt is that NO oxidation activity decreases with decreasing Pt particle size but accelerates when Pt is present only as single atoms.

Hydrogenation and dehydrogenation reactions

In addition to oxidations, SACs have been widely used in various hydrogenation and dehydrogenation reactions, such as hydrogenation of nitroarenes (Wei et al. 2014), styrene (Kyriakou et al. 2012), acetylene (Guang et al. 2017a, b; Guang et al. 2015; Pei et al. 2014), 1,3-butadiene (Huan et al. 2015; Zhang et al. 2005), 1-hexyne (Gianvito et al. 2015), acrolein (Aich et al. 2015), alkynol (Crespo-Quesada et al. 2011), 3-nitrostyrene (Wei et al. 2014), and dehydrogenation of formic acid (Matthew et al. 2017; Cao et al. 2015a, b), and propane (Matthew et al. 2017). SACs have exhibited impressive catalytic performances. For example, by anchoring individual Pd atoms onto highly porous C_3N_4, an excellent and thermally stable catalyst was synthesized and used to perform catalytic hydrogenations including the conversion of 1-hexyne to 1-hexene, selectively converting the C≡C triple bonds without degrading the C≡C double bonds (Fig. 19) (Huan

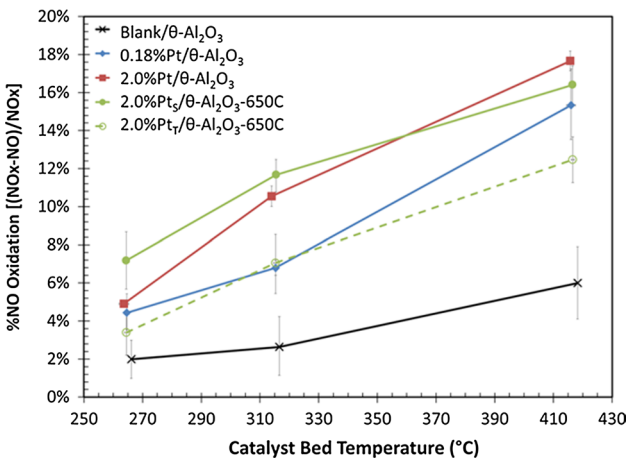

Fig. 18 Steady-state plots of average NO oxidation to NO_2 for blank θ-Al_2O_3 and catalysts 0.18%Pt/θ-Al_2O_3, 2.0%Pt/θ-Al_2O_3, 2.0%Pt_S/θ-Al_2O_3-650C, and 2.0%Pt_T/θ-Al_2O_3-650C. Error bars indicate min/max values. Adapted from Narula et al. (2014)

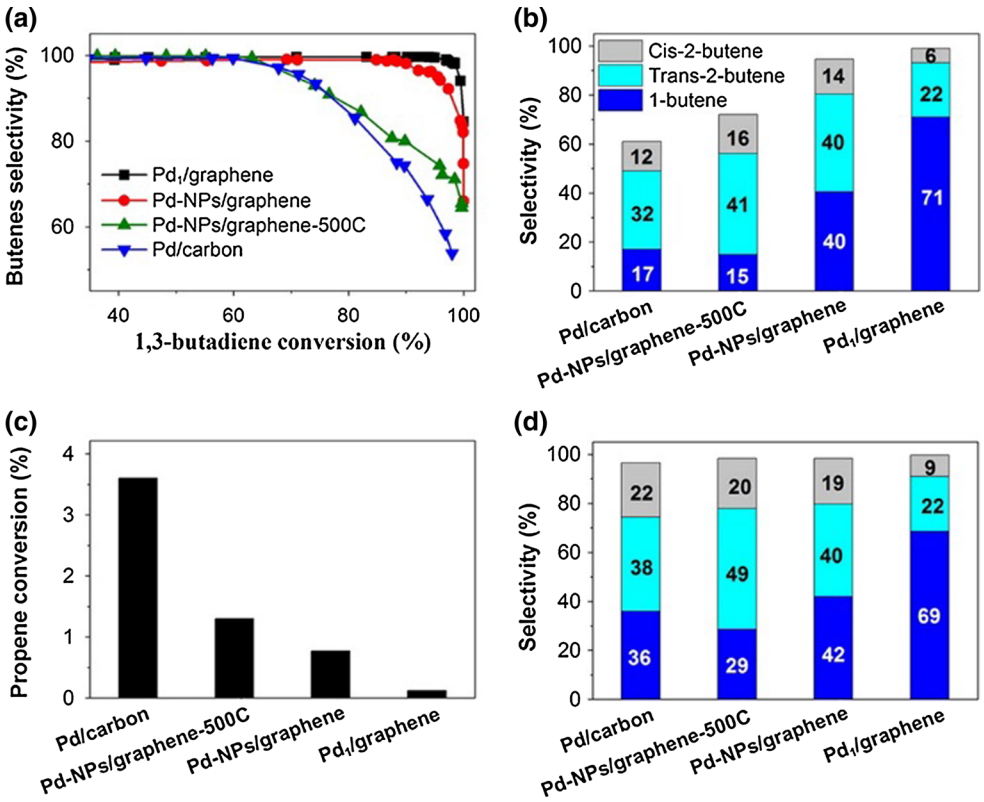

Fig. 19 Catalytic performances of Pd_1/graphene, Pd-NPs/graphene, Pd-NPs/graphene-500C, and Pd/carbon samples in selective hydrogenation of 1,3-butadiene. **a** Butenes selectivity as a function of conversion by changing the reaction temperatures; **b** distribution of butenes at 95% conversion. Propene conversion (**c**) and distribution of butenes (**d**) at 98% 1,3-butadiene conversion in hydrogenation of 1,3-butadiene in the presence of propene. Adapted from Huan et al. (2015)

et al. 2015). By placing isolated Pd atoms on a Cu surface, one can substantially lower the energy barrier to both dissociation of H_2 molecules on Pd atoms and the subsequent desorption of the product molecules from the Cu metal surface (Guang et al. 2017a, b). Such a facile hydrogen dissociation on Pd atom sites, spilling over to Cu sites, and weak binding of Cu to the product molecules allow for selective hydrogenation of styrene and acetylene compared to using pure Cu or Pd metal alone. By stabilizing single Pt atoms on FeO_x support, highly active, chemoselective, and reusable catalysts was obtained for the hydrogenation of various nitroarenes (Wei et al. 2014). For hydrogenation of 3-nitrostyrene, the catalyst yields a turnover frequency of ~ 1500 h^{-1}, which is 20 times higher than the best result reported in the literature, and a selectivity to 3-aminostyrene close to 99%, the best result ever achieved over platinum group metals. The superior performance can be attributed to the presence of positively charged platinum centers and the absence of Pt-t metallic bonding, both of which favor the preferential desorption of nitro groups. The design of a series of Cu-supported Pt SACs and the application of these to the selective hydrogenation of 1,3-butadiene to 1-butene are further proof of the unique catalytic applications of manipulating atomic species to achieve desired catalytic reactions (Lucci et al. 2015).

Water–gas shift reaction (WGS)

The WGS reaction ($CO + H_2O \rightarrow CO_2 + H_2$), which is of great significance in producing H_2-rich fuel gas streams for fuel cell and other applications, has been shown to occur on single metal atoms (Kunlun et al. 2015; Yang et al. 2013a, b; Sara et al. 2014; Hongling et al. 2017; Sun et al. 2017; Flytzani-Stephanopoulos 2014; Yang et al. 2015; Yang and Flytzani-Stephanopoulos 2017). Zhang et al. reported the preparation and characterization of Ir_1/FeO_x SAC, the activity of which is 10 times higher than its cluster or nanoparticle counterparts and is even higher than those of the most active Au- or Pt-based catalysts (Lin et al. 2013a, b). The Ir single atoms seem to greatly enhance the reducibility of FeO_x s and generation of oxygen vacancies, leading to the excellent performance of the Ir_1/FeO_x SAC for WGS. Flytzani-Stephanopoulos research group has devoted interests to the investigation of catalysts with isolated single sites for the WGS reaction (Yang et al. 2013a, b, 2015; Flytzani-Stephanopoulos 2014; Fu et al. 2003). They proposed that the intrinsic activity of the M_1–O_x (OH)–S site, where M_1 is a metal ion and S is a support, is the same for any support. The support effect is indirect, through its carrying or binding capacity for the active sites. Heyden et al. reported that a positively charged single Pt atom on TiO_2 (110) can exhibit a very

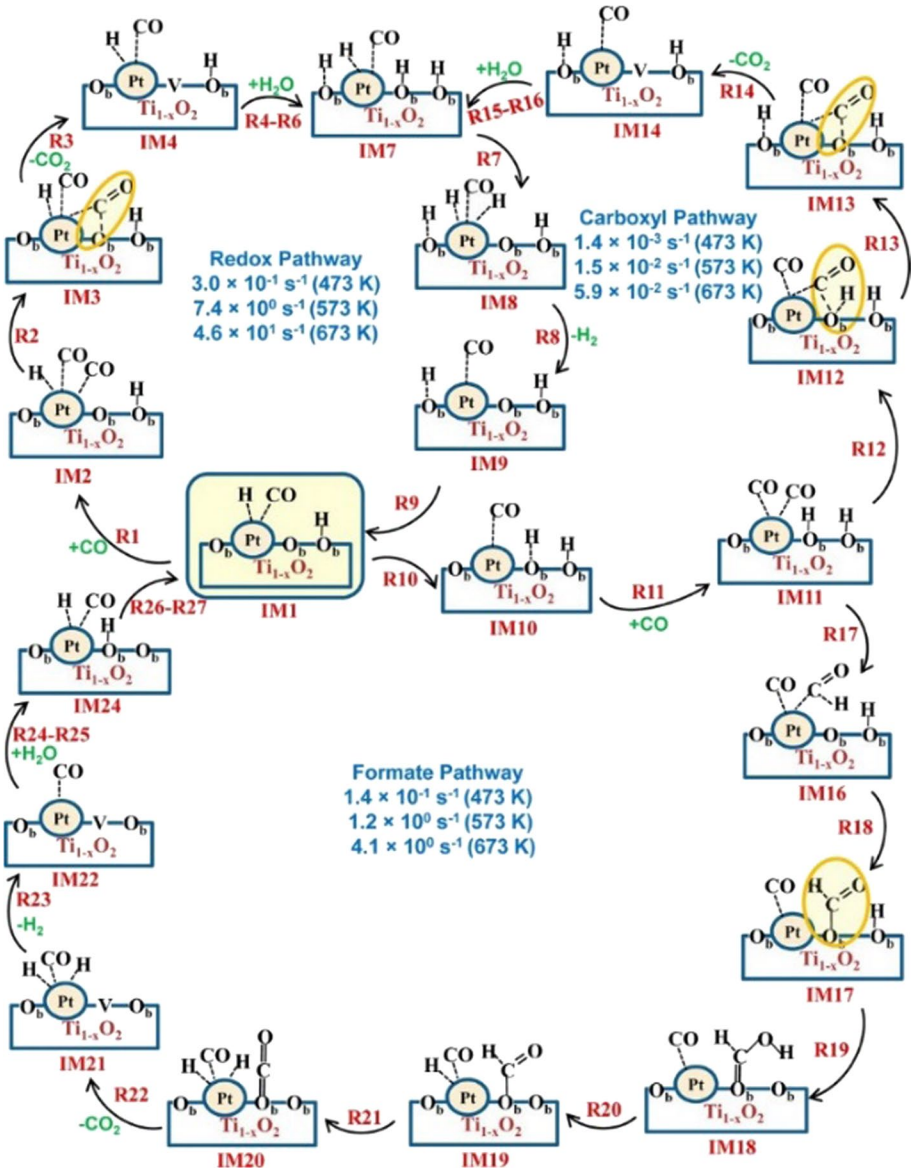

Fig. 20 Reaction network of various WGS reaction steps on a positively charged Pt atom supported on a $Ti_{1-x}O_2$ (110) surface. Adapted from Sara et al. (2014)

high activity for the WGS reaction under low temperature (Salai and Andreas 2017).

Possible reaction pathways for the WGS are proposed, containing the redox, associative carboxyl, and formate pathways (Fig. 20). The classical redox pathway is the dominant pathway in the temperature range of 473–673 K and that high turnover frequencies are possible for this active site. The formate pathway with redox regeneration is preferred over the carboxyl pathway with redox regeneration, and its rate is very close to that of the classical redox pathway at temperatures below 573 K. Single Pt^{2+} sites stabilized on a reducible surface such as TiO_2 (110) are active for the WGS at low temperatures, where the formation of oxygen vacancies on the TiO_2 surface plays a significant role in the WGS activity. Furthermore, the single Pt^{2+} sites stabilized on TiO_2 (110) with CO and H as ligands exhibit characteristics similar to those of homogeneous catalysts and, thus, can possess the combined advantages of both homogeneous and heterogeneous catalysts.

Reforming reactions

Gu et al. prepared the supported single Pt_1/Au_1 atoms for methanol steam reforming (Xiang-Kui et al. 2014). The isolated precious metal atoms including Pt_1 and Au_1 together with coordinated lattice oxygen embedded onto ZnO surfaces provide single, stable active sites for methanol steam reforming. DFT calculations revealed that the catalysis of the single precious metal atoms with coordinated lattice oxygen stems from their stronger binding toward the intermediates, lowering reaction barriers, changing on the reaction pathway, and thus enhancing the activity (Fig. 21). The

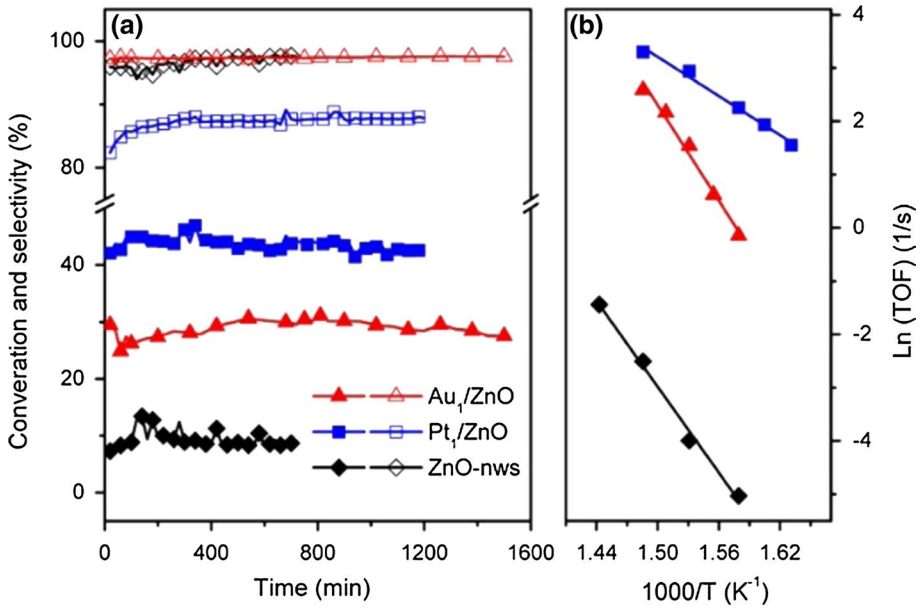

Fig. 21 **a** Methanol conversion (solid) and CO_2 selectivity (open) as a function of reaction time at 390 °C on Au_1/ZnO (red triangle), Pt_1/ZnO (blue square) catalysts, and the pristine ZnO nanowires (black diamond); **b** corresponding Arrhenius plots of the reaction rate Ln (TOF) (s^{-1}) versus 1/*T* for the MSR reaction. Adapted from Xiang-Kui et al. (2014)

measured turnover frequency of single Pt_1 sites was three orders of magnitude higher than the pristine ZnO. Besides, the activity of the Pt_1/ZnO is much higher than that of the Au_1/ZnO, and the CO selectivity of the Pt_1/ZnO is very different from that of the Au_1/ZnO as well, clearly demonstrating that the performance of the metal SACs strongly depends on the right combination of the metal and the support.

Electrocatalysis

Electrocatalysis, as a branch of heterogeneous catalysis, mainly occurs at the solid–liquid interface, where reactants accept or lose electrons at the cathode or anode reaction, respectively. Besides surface configuration, chemical composition, and electronic structure, some other important issues such as material conductivity, bi-continuity, and solvent effects must be taken into consideration when designing electrocatalysts, which ought to be stable enough when continuously working in practical conditions. SACs have been intensively studied for some heterogeneously catalyzed reactions, as mentioned above. The high activity and selectivity of SACs are desirable for electrocatalysis and instability issues could be alleviated when single atoms are tightly anchored to the host matrix (Zhu et al. 2017; Liang et al. 2017a, b).

One example of the use of SAC in electrocatalysis was reported in 2015 by Fei et al. in which the SAC was prepared by deposition of Pt atoms on N-doped graphene. The SAC has been proved to be an effective and durable catalyst for the electrocatalytic water splitting reaction in both acid and base media (Fei et al. 2015). The electrocatalytic performance of the Co_1/N-doped graphene proved to be excellent with an intrinsic activity per Co atom. The Co–N interaction is critical to creating the Co–N active sites. This excellent catalytic performance, maximal efficiency of atomic utility, scalability, and low cost for the preparation make this catalyst a promising candidate for water splitting applications. Shi et al. demonstrated the use of Pt_1/FeO_x in photovoltaics, as the counter electrode (CE) in dye-sensitized solar cells (DSCs) (Yantao et al. 2014). Compared with conventional CEs, the SAC-based CE exhibited much better activity and reversibility for the catalytic reduction of triiodide (I_3^-) into iodide (I^-). Pt_1/FeO_x with an 0.08 wt% Pt loading exhibited effective atom utilization, and the PCE of its DSCs is double that of bare FeO_x-based DSCs. Using such Pt_1/FeO_x, high PCEs of up to 9.03% were achieved, approaching that of 9.44%, which has been achieved by DSCs based on sputtering Pt. Additionally, Pt_1/FeO_x exhibited good stability in the liquid electrolyte system of DSCs. By preparing highly porous zeolite-templated carbon with large amounts of S functionalities (17 wt%) and highly curved three-dimensional networks of graphene nanoribbons, high loading levels of Pt single atoms (5 wt%) have been achieved (Choi et al. 2016). In the oxygen reduction reaction, the atomically dispersed Pt catalyst selectively catalyzes a two-electron oxygen reduction reaction (ORR) pathway producing H_2O_2, rather than the conventional four-electron ORR pathway producing H_2O (Fig. 22).

Photocatalysis

The research and applications of SACs are rapidly being extended. In 2014, Yang and co-workers for the first time reported the use of SACs of M_1/TiO_2 in photocatalytic hydrogen evolution, where M is an isolated atom of Pt, Pd, Rh, or Ru strongly anchored to the support (Xing

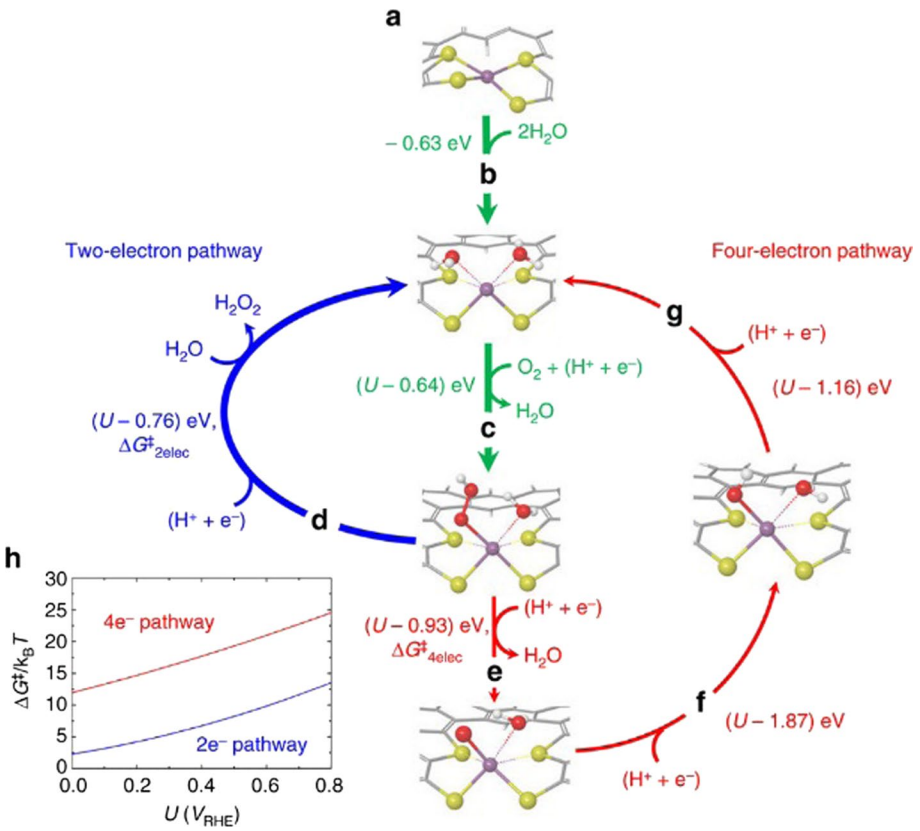

Fig. 22 (a) Atomically dispersed Pt (purple) complexed with four sulfur-containing moieties consisting of two thiophene and two thiolate groups that are covalently bonded to a carbon framework. (b) Activation of the Pt center by substituting two S of thiophene-like moieties with two O of water molecules. (c) First reduction of an O_2 via proton-coupled electron transfer (PCET), forming OOH. This is a shared elementary step of the two- and four-electron pathways. (d) Two-electron pathway: H_2O_2 formation by the second PCET and the subsequent substitution of an H_2O_2 molecule with an outer-sphere H_2O molecule, recovering the initial state where Pt is complexed with two thiolates and two waters. (e) Four-electron pathway: H_2O formation by the second PCET involving O–O bond dissociation. (f) Four-electron pathway: OH formation by the third PCET to the O atom. (g) Fourth PCET to the OH forms an inner-sphere H_2O, recovering the initial state where Pt is complexed with two thiolates and two waters. (h) Calculated kinetic barriers of the second PCET steps for the two-electron pathway (blue) and the four-electron pathway (red) using Marcus kinetic theory. (C: gray, H: white, S: yellow, O: red, and Pt: purple). Adapted from Choi et al. (2016)

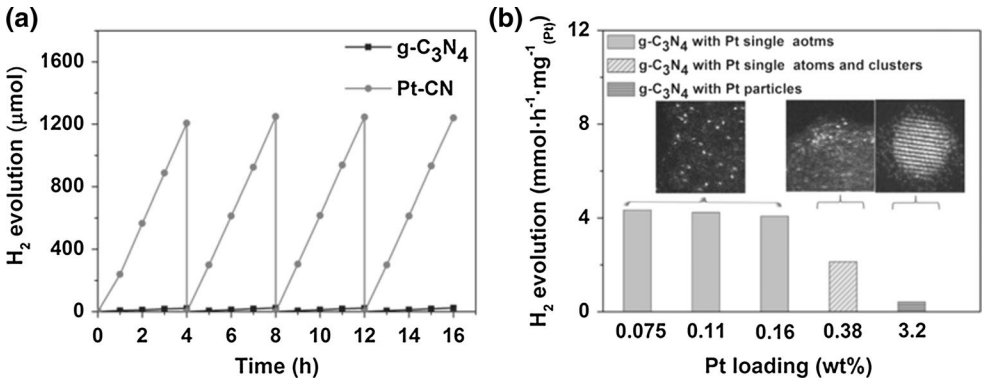

Fig. 23 Photocatalytic H_2 evolution performance. **a** Photocatalytic H_2 generation activity of g-C_3N_4 and Pt-CN. **b** Photocatalytic activity comparison of g-C_3N_4 with various Pt contents normalized to per Pt atom. Adapted from Xiaogang et al. (2016)

et al. 2014). As novel photocatalysts, M_1/TiO_2 illustrated not only excellent stability for H_2 evolution, but also a 6–13-fold increase in photocatalytic activity compared with the metal clusters loaded onto TiO_2. By embedding Pt single atoms into 2D porous g-C_3N_4 as co-catalyst, a remarkable performance for photocatalytic H_2 evolution has been realized, which is 8.6 times higher than that of Pt nanoparticles and nearly 50 times of that for bare g-C_3N_4

(in Fig. 23) (Xiaogang et al. 2016). The cooperation of single-atom Pt in g-C_3N_4 provides a new strategy to modulate the electronic structure, resulting in a longer lifetime of photogenerated electrons due to the isolated single Pt atoms induced, intrinsic change in the surface trap states, eventually leads to tremendously enhanced photocatalytic H_2 generation performance. It was believed that the single-atom co-catalyst strategy will provide a promising way to reduce the high cost of noble metals and pave a new avenue for the development of highly efficient co-catalysts.

Summary and prospective

The utilization of SACs provides vast opportunities for applications in heterogeneous catalysis. SACs not only improve the utilization efficiency of metals but also provide an alternative strategy to tune the activity and selectivity of catalytic reactions. It is very encouraging that our understanding of SACs has been further promoted thanks to substantial works on sample preparation, characterization, and mechanism interpretation. Various synthetic methods including the mass-selected soft-landing technique, ALD, wet chemistry, and other methods have been developed to prepare supported SACs. This wide range of techniques has enabled the demonstration of SACs on a wide range of support materials. Advanced characterization techniques such as STEM, AFM, EXAFS, XANES, DRIFTS, and NMR, along with the theoretical DFT calculations, have been used to study SACs. These techniques have proved invaluable for verifying the atomic nature of the catalysts and preferred binding sites. However, great challenges remain, including controllable and facile preparation of SACs, robust stabilization of the single atoms on the support, comprehensive understanding and tuning of the SMSIs, and rational and precise design of active sites in SACs. More efforts are needed from synthesis to properties and practical applications of SACs. It is expected that with innovative synthetic strategies, advanced characterization tools, and theoretical calculations we can make significant progress in understanding the fundamental properties of supported single metal atoms and realize the ultimate goal of manipulating individual atoms for function.

Acknowledgements We gratefully acknowledge financial support from the National Nature Science Foundation of China (Grant No. 21473248), the CAS/SAFEA International Partnership Program for Creative Research Teams, and the National Science Foundation under Grant #IIP-1059286 to the American Society for Engineering Education. All individual contributions in the cited references are gratefully acknowledged, and any omission is regretted.

References

Abbet AS, Heiz U, Schneider WD, Ferrari AM, Pacchioni G, Rolsch N (2000) Acetylene cyclotrimerization on supported size-selected Pd_n clusters ($1 < n < 30$): one atom is enough! J Am Chem Soc 122:3453–3457. https://doi.org/10.1021/ja9922476

Aich P, Wei H, Basan B, Kropf AJ, Schweitzer NM, Marshall CL, Miller JT, Meyer R (2015) Single-atom alloy Pd–Ag catalyst for selective hydrogenation of acrolein. J Phys Chem C 119:18140–18148. https://doi.org/10.1021/acs.jpcc.5b01357

Albert B, Yaroslava L, Iva M, Armin N, Tomas S, Nataliya T, Mykhailo V, Vitalii S, Klara S, Josef M, Roman F, Michal V, Kevin CP, Stephanie B, Valerie P, Francesc I, Vladimr M, Jçrg L, Konstantin MN (2014) Maximum noble-metal efficiency in catalytic materials: atomically dispersed surface platinum. Angew Chem Int Ed 53:10525–10530. https://doi.org/10.1002/anie.201402342

Aleksandrov HA, Neyman KM, Vayssilov GN (2015) The structure and stability of reduced and oxidized mononuclear platinum species on nanostructured ceria from density functional modeling. Phys Chem Chem Phys 17:14551–14560. https://doi.org/10.1039/c5cp01685a

Alex WR, Yung-Chang L, Shanshan W, Hidetaka S, Christopher SA, Qu C, Sungwoo L, Gun DL, Joohee L, Seungwu H, Euijoon Y, Angus IK, Heeyeon K, Kazu S, Jamie HW (2016) Atomic structure and spectroscopy of single metal (Cr, V) substitutional dopants in monolayer MoS_2. ACS Nano 10:10227–10236. https://doi.org/10.1021/acsnano.6b05674

Alexeev O, Gates BC (2000) EXAFs characterization of supported metal-complex and metal-cluster catalysts made from organometallic precursors. Top Catal 10:273–293. https://doi.org/10.1023/a:1019184605678

Benjamin ES, Jennifer KE, Philip L, Albert FC, Andrew H, Christopher JK, Hutchings Graham J (2006) Direct synthesis of hydrogen peroxide from H_2 and O_2 using Al_2O_3 supported Au–Pd catalysts. Chem Mater 18:2689–2695. https://doi.org/10.1021/cm052633o

Benjamin M, Henry CA, Chaohui G, Sandy MK, Perrin ES, Jennifer MR, Howie C, Richard WB, Daniel IG (2016) Tail use improves performance on soft substrates in models of early vertebrate land locomotors. Science 353:154–159. https://doi.org/10.1126/science.aaf0984

Bing H, Botao Q, Aiqin W, Tao Z (2017) Highlights of the major progress in single-atom catalysis in 2015 and 2016. Chin J Catal. https://doi.org/10.1016/S1872-2067(17)62872-9

Botao Q, Jiaxin L, Yang-Gang W, Qingquan L, Xiaoyan L, Aiqin W, Jun L, Tao Z, Jingyue L (2015) Highly efficient catalysis of preferential oxidation of CO in H_2-rich stream by gold single-atom catalysts. ACS Catal 5:6249–6254. https://doi.org/10.1021/acscatal.5b01114

Cao X, Fu Q, Luo Y (2014) Catalytic activity of Pd-doped cu nanoparticles for hydrogenation as a single-atom-alloy catalyst. Phys Chem Chem Phys 16:8367–8375. https://doi.org/10.1039/c4cp00399c

Cao X, Mirjalili A, Wheeler J, Xie W, Jang BWL (2015a) Investigation of the preparation methodologies of Pd–Cu single atom alloy catalysts for selective hydrogenation of acetylene. Front Chem Sci Eng 9:442–449. https://doi.org/10.1007/s11705-015-1547-x

Cao X, Ji Y, Luo Y (2015b) Dehydrogenation of propane to propylene by a Pd/Cu single-atom catalyst: insight from first-principles calculations. J Phys Chem C 119:1016–1023. https://doi.org/10.1021/jp508625b

Cavanagh RR, Yates JT (1981) Site distribution studies of Rh supported on Al_2O_3-an infrared study of chemisorbed CO. J Chem Phys 74:4150–4155. https://doi.org/10.1063/1.441544

Chen MS (2004) The structure of catalytically active gold on titania. Science 306:252–255. https://doi.org/10.1126/science.1102420

Cheng MJC, Ezra LP, Hieu HB, Alexis TH (2016a) Quantum mechanical screening of single-atom bimetallic alloys for the selective reduction of CO_2 to C_1 hydrocarbons. ACS Catal 6:7769–7777. https://doi.org/10.1021/acscatal.6b01393

Cheng N, Stambula S, Wang D, Banis MN, Liu J, Riese A, Xiao B, Li R, Sham TK, Liu LM, Botton GA, Sun X (2016b) Platinum single-atom and cluster catalysis of the hydrogen evolution reaction. Nat Commun 7:13638. https://doi.org/10.1038/ncomms13638

Chithra A, DeRita L, Phillip C (2017) Using probe molecule ftir spectroscopy to identify and characterize Pt-group metal based single atom catalysts. Chin J Catal 38:1473–1480. https://doi.org/10.1016/S1872-2067(17)62876-6

Choi CH, Kim M, Kwon HC, Cho SJ, Yun S, Kim HT, Mayrhofer KJ, Kim H, Choi M (2016) Tuning selectivity of electrochemical reactions by atomically dispersed platinum catalyst. Nat Commun 7:10922–10930. https://doi.org/10.1038/ncomms10922

Chunlei W, Xiang-Kui G, Huan Y, Yue L, Junjie L, Dandan L, Wei-Xue L, Junling L (2017) Water-mediated Mars–Van Krevelen mechanism for CO oxidation on ceria-supported single-atom Pt_1 catalyst. ACS Catal 7:887–891. https://doi.org/10.1021/acscatal.6b02685

Corma A, Salnikov OG, Barskiy DA, Kovtunov KV, Koptyug IV (2015) Single-atom gold catalysis in the context of developments in parahydrogen-induced polarization. Chem Eur J 21:7012–7015. https://doi.org/10.1002/chem.201406664

Crespo-Quesada M, Artur Y, Jin MS, Xia Y, Lioubov K (2011) Structure sensitivity of alkynol hydrogenation on shape- and size-controlled palladium nanocrystals: which sites are most active and selective? J Am Chem Soc 133:12787–12794. https://doi.org/10.1021/ja204557m

Daniel M, Heron V, Lorenzo R, Stfephane F, Xile H (2012) Fe Co, and Ni ions promote the catalytic activity of amorphous molybdenum sulfide films for hydrogen evolution. Chem Sci 3:2515–2525. https://doi.org/10.1039/c2sc20539d

Deng Q, Zhao L, Gao X, Zhang M, Luo Y, Zhao Y (2013) Single layer of polymeric cobalt phthalocyanine: promising low-cost and high-activity nanocatalysts for co oxidation. Small 9:3506–3513. https://doi.org/10.1002/smll.201300652

Ding WC, Gu XK, Su HY, Li WX (2014) Single Pd atom embedded in CeO_2(111) for NO reduction with CO: a first-principles study. J Phys Chem C 118:12216–12223. https://doi.org/10.1021/jp503745c

Ding K, Gulec A, Alexis MJ, Neil MS, Galen DS, Laurence DM, Peter CS (2015) Identification of active sites in CO oxidation and water–gas shift over supported Pt catalysts. Science 350:189–192. https://doi.org/10.1126/science.aac6368

Dmitri AB, Monika Z, Alexander SL, Olga YP, Fredrik SH, Quentin MR, Ursel B, Lyubov GB (2016) Single atoms of Pt-group metals stabilized by *n*-doped carbon nanofibers for efficient hydrogen production from formic acid. ACS Catal 6:3442–3451. https://doi.org/10.1021/acscatal.6b00476

Du C, Lin H, Lin B, Ma Z, Hou T, Tang J, Li Y (2015) MoS_2 supported single platinum atoms and their superior catalytic activity for CO oxidation: a density functional theory study. J Mater Chem A 3:23113–23119. https://doi.org/10.1039/c5ta05084g

Dvořák F, Farnesi CM, Tovt A, Tran ND, Negreiros FR, Vorokhta M, Skála T, Matolínová I, Mysliveček J, Matolín V, Fabris S (2016) Creating single-atom Pt-ceria catalysts by surface step decoration. Nat Commun 7:10801–10808. https://doi.org/10.1038/ncomms10801

Edwards J, Solsona B, Landon P, Carley A, Herzing A, Kiely C, Hutchings G (2005) Direct synthesis of hydrogen peroxide from H_2 and O_2 using TiO_2-supported Au–Pd catalysts. J Catal 236:69–79. https://doi.org/10.1016/j.jcat.2005.09.015

Enache DI (2006) Solvent-free oxidation of primary alcohols to aldehydes using Au–Pd/TiO_2 catalysts. Science 311:362–365. https://doi.org/10.1126/science.1120560

Ewing CS, Bagusetty A, Patriarca EG, Lambrecht DS, Veser G, Johnson JK (2016) Impact of support interactions for single-atom molybdenum catalysts on amorphous silica. Ind Eng Chem Res 55:12350–12357. https://doi.org/10.1021/acs.iecr.6b03558

Fei H, Dong J, Arellano-Jimenez MJ, Ye G, Dong KN, Samuel EL, Peng Z, Zhu Z, Qin F, Bao J, Yacaman MJ, Ajayan PM, Chen D, Tour JM (2015) Atomic cobalt on nitrogen-doped graphene for hydrogen generation. Nat Commun 6:8668–8675. https://doi.org/10.1038/ncomms9668

Fengyu L, Yafei L, Xiao CZ, Zhongfang C (2015) Exploration of high-performance single-atom catalysts on support M_1/FeO_x for co oxidation via computational study. ACS Catal 5:544–552. https://doi.org/10.1021/cs501790v

Figueroba A, Kovács G, Bruix A, Neyman KM (2016) Towards stable single-atom catalysts: strong binding of atomically dispersed transition metals on the surface of nanostructured ceria. Catal Sci Technol 6:6806–6813. https://doi.org/10.1039/c6cy00294c

Flytzani-Stephanopoulos M (2014) Gold atoms stabilized on various supports catalyze the water–gas shift reaction. Acc Chem Res 47:783–792. https://doi.org/10.1021/ar4001845

Fu Q, Saltsburg H, Maria F (2003) Active nonmetallic Au and Pt species on ceria-based water–gas shift catalysts. Science 301:935–939. https://doi.org/10.1126/science.1085721

Gai PL, Yoshida K, Ward, Walsh M, Baker RT, Van De Water L, Watson MJ, Boyes ED (2016) Visualisation of single atom dynamics in water gas shift reaction for hydrogen generation. Catal Sci Technol 6:2214–2227. https://doi.org/10.1039/c5cy01154j

Gao H (2016) CO oxidation mechanism on the γ-Al_2O_3 supported single Pt atom: first principle study. Appl Surf Sci 379:347–357. https://doi.org/10.1016/j.apsusc.2016.04.009

Gao M, Lyalin A, Taketsugu T (2013) Co oxidation on h-BN supported Au atom. J Chem Phys 138:034701–034709. https://doi.org/10.1063/1.4774216

Gao G, Jiao Y, Waclawik ER, Du A (2016) Single atom (Pd/Pt) supported on graphitic carbon nitride as an efficient photocatalyst for visible-light reduction of carbon dioxide. J Am Chem Soc 138:6292–6297. https://doi.org/10.1021/jacs.6b02692

Gates BC (1995) Supported metal clusters: synthesis, structure, and catalysis. Chem Rev 95:511–522. https://doi.org/10.1021/cr00035a003

Ghosh TK, Nair NN (2013) Rh_1/γ-Al_2O_3 single-atom catalysis of O_2 activation and CO oxidation: mechanism, effects of hydration, oxidation state, and cluster size. ChemCatChem 5:1811–1821. https://doi.org/10.1002/cctc.201200799

Gianvito V, Davide A, Maarten N, Zupeng C, Dariya D, Markus A, Núria L, Javier P (2015) A stable single-site palladium catalyst for hydrogenations. Angew Chem Int Ed 54:11265–11269. https://doi.org/10.1002/anie.201505073

Greecor RB, Lytle FW (1980) Morphology of supported metal clusters: determination by EXAFs and chemisorption. J Catal 63:476–486. https://doi.org/10.1016/0021-9517(80)90102-5

Guang XP, Xiao YL, Aiqin W, Adam FL, Mark AI, Lin L, Xiaoli P, Xiaofeng Y, Xiaodong W, Zhijun T, Karen W, Tao Z (2015) Ag alloyed Pd single-atom catalysts for efficient selective hydrogenation of acetylene to ethylene in excess ethylene. ACS Catal 5:3717–3725. https://doi.org/10.1021/acscatal.5b00700

Guang XP, Xiao YL, Xiaofeng Y, Leilei Z, Aiqin W, Lin L, Hua W, Xiaodong W, Tao Z (2017a) Performance of Cu-alloyed pd single-atom catalyst for semihydrogenation of acetylene under simulated front-end conditions. ACS Catal 7:1491–1500. https://doi.org/10.1021/acscatal.6b03293

Guang X, Pei XY, Meng L, Qian C, Aiqin W, Tao Z (2017b) Isolation of Pd atoms by Cu for semi-hydrogenation of acetylene: effects of

Cu loading. Chin J Catal 38:1540–1548. https://doi.org/10.1016/S1872-2067(17)62847-X

Guo X, Fang G, Li G, Ma H, Fan H, Yu L, Ma C, Wu X, Deng D, Wei M, Tan D, Si R, Zhang S, Li J, Sun L, Tang Z, Pan X, Bao X (2014) Direct, nonoxidative conversion of methane to ethylene, aromatics, and hydrogen. Science 344:616–619. https://doi.org/10.1126/science.1253150

Hao Z, Geng W, Da Ch, Xiaojun L, Jinghong L (2008) Tuning photoelectrochemical performances of Ag–TiO_2 nanocomposites via reduction/oxidation of Ag. Chem Mater 20:6543–6549. https://doi.org/10.1021/cm801796q

He H, Jagvaral Y (2017) Electrochemical reduction of CO_2 on graphene supported transition metals—towards single atom catalysts. Phys Chem Chem Phys 19:11436–11446. https://doi.org/10.1039/c7cp00915a

Heiz U, Sanchez A, Abbet S, Schneider WD (1999) Catalytic oxidation of carbon monoxide on monodispersed platinum clusters-each atom counts. J Am Chem Soc 121:3214–3217. https://doi.org/10.1021/ja983616l

Hongling G, Tao Z, Jian L, Botao Q, Shu M, Aiqin W, Xiao D (2017) Enhanced performance of Rh_1/TiO_2 catalyst without methanation in water–gas shift reaction. AIChE J 63:2081–2088. https://doi.org/10.1002/aic.15585

Huan Y, Hao C, Hong Y, Yue L, Tao Y, Wang C, Li J, Wei S, Lu J (2015) Single-atom Pd_1/graphene catalyst achieved by atomic layer deposition: remarkable performance in selective hydrogenation of 1,3-butadiene. J Am Chem Soc 137:10484–10487. https://doi.org/10.1021/jacs.5b06485

Huang X, Xia Y, Cao Y, Zheng X, Pan H, Zhu J, Ma C, Wang H, Li J, You R, Wei S, Huang W, Lu J (2017) Enhancing both selectivity and coking-resistance of a single-atom Pd_1/C_3N_4 catalyst for acetylene hydrogenation. Nano Res 10:1302–1312. https://doi.org/10.1007/s12274-016-1416-z

Ja HK, Jianzhi H, Donghai M, Cheol-Woo Y, Do HK, Charles HFP, Lawrence FA, Janos S (2009) Coordinatively unsaturated Al^{3+} centers as binding sites for active catalyst phases of platinum on γ-Al_2O_3. Science 325:1670–1674. https://doi.org/10.1126/science.1176745

Jia H, Wang C (2015) Dechlorination of chlorinated phenols by subnanoscale Pd^0/Fe^0 intercalated in smectite: pathway, reactivity, and selectivity. J Hazard Mater 300:779–787. https://doi.org/10.1016/j.jhazmat.2015.08.017

Jinxia L, Congqiao X, Tao Z, Jun L (2017) Catalytic activities of single-atom catalysts for CO oxidation: Pt_1/FeO_x vs. Fe_1/FeO_x. Chin J Catal 38:1566–1573. https://doi.org/10.1016/S1872-2067(17)62879-1

Jirkovsky JS, Panas I, Ahlberg E, Halasa M, Romani S, Schiffrin DJ (2011) Single atom hot-spots at Au–Pd nanoalloys for electrocatalytic H_2O_2 production. J Am Chem Soc 133:19432–19441. https://doi.org/10.1021/ja206477z

John J, Haifeng X, Andrew TD, Eric JP, Hien P, Sivakumar RC, Gongshin Q, Se O, Michelle HW, Xavier IPH, Yong W, Abhaya KD (2016) Thermally stable single-atom platinum-on-ceria catalysts via atom trapping. Science 353:150–154. https://doi.org/10.1126/science.aaf8800

Joseph D, Kistler NC, Pinghong X, Bryan E, Piyasan P, Cong-Yan C, Nigel DB, Bruce CG (2014) A single-site platinum CO oxidation catalyst in zeolite KLTL: microscopic and spectroscopic determination of the locations of the platinum atoms. Angew Chem Int Ed 53:8904–8907. https://doi.org/10.1002/anie.201403353

Kaden WE, Wu T, Kunkel WA, Anderson SL (2009) Electronic structure controls reactivity of size-selected Pd clusters adsorbed on TiO_2 surfaces. Science 326:826–829. https://doi.org/10.1126/science.1180297

Kesavan L, Tiruvalam R, Rahim MHA, Bin Saiman MI, Enache DI, Jenkins RL, Dimitratos N, Lopez-Sanchez JA, Taylor SH, Knight DW, Kiely CJ, Hutchings GJ (2011) Solvent-free oxidation of primary carbon-hydrogen bonds in toluene using Au–Pd alloy nanoparticles. Science 331:195–199. https://doi.org/10.1126/science.1198458

Kunlun D, Ahmet G, Alexis MJ, Neil MS, Galen DS, Laurence DM, Peter CS (2015) Identification of active sites in co oxidation and water–gas shift over supported Pt catalysts. Science 350:189–192. https://doi.org/10.1126/science.aac6368

Kuo L, Aipin W, Zhang Tao (2012) Recent advances in preferential oxidation of CO reaction over platinum group metal catalysts. ACS Catal 2:1165–1178. https://doi.org/10.1021/cs200418w

Kwang TR, Daejin E, Li L, Elena S, Joan MR, Siu-Wai C, Maria F, George WF (2009) Charging and chemical reactivity of gold nanoparticles and adatoms on the (111) surface of single-crystal magnetite: a scanning tunneling microscopy/spectroscopy study. J Phys Chem C 113:10198–10205. https://doi.org/10.1021/jp8112599

Kyriakou G, Boucher MB, Jewell AD, Lewis EA, Lawton TJ, Baber AE, Tierney HL, Flytzani-Stephanopoulos M, Sykes ECH (2012) Isolated metal atom geometries as a strategy for selective heterogeneous hydrogenations. Science 335:1209–1212. https://doi.org/10.1126/science.1215864

Lang R, Li T, Matsumura D, Miao S, Ren Y, Cui YT, Tan Y, Qiao B, Li L, Wang A, Wang X, Zhang T (2016) Hydroformylation of olefins by a rhodium single-atom catalyst with activity comparable to RhCl(PPh3)3. Angew Chem Int Ed 55:16054–16058. https://doi.org/10.1002/anie.201607885

Lei Y, Mehmood F, Lee S, Greeley J, Lee B, Seifert S, Winans RE, Elam JW, Meyer RJ, Redfern PC, Teschner D, Schlogl R, Pellin MJ, Curtiss LA, Vajda S (2010) Increased silver activity for direct propylene epoxidation via subnanometer size effects. Science 328:224–228. https://doi.org/10.1126/science.1185200

Leilei Z, Jeffrey TM, Xiaoyan L, Xiaofeng Y, Wentao W, Lin L, Yanqiang H, Chung-Yuan M, Tao Z (2014) Efficient and durable Au alloyed pd single-atom catalyst for the Ullmann reaction of aryl chlorides in water. ACS Catal 4:1546–1553. https://doi.org/10.1021/cs500071c

Li C (2016) Single Co atom catalyst stabilized in C/N containing matrix. Chin J Catal 37:1443–1445. https://doi.org/10.1016/s1872-2067(16)62520-2

Li Y, Sun Q (2014) The superior catalytic CO oxidation capacity of a Cr-phthalocyanine porous sheet. Sci Rep 4:4098–4104. https://doi.org/10.1038/srep04098

Li ZY, Yuan Z, Li XN, Zhao YX, He SG (2014) CO oxidation catalyzed by single gold atoms supported on aluminum oxide clusters. J Am Chem Soc 136:14307–14313. https://doi.org/10.1021/ja508547z

Li F, Li L, Liu X, Zeng XC, Chen Z (2016) High-performance Ru_1/CeO_2 single-atom catalyst for CO oxidation: a computational exploration. ChemPhysChem 17:3170–3175. https://doi.org/10.1002/cphc.201600540

Li Q, Ma Z, Sa R, Adidharma H, Gasem KAM, Russell AG, Fan M, Wu K (2017) Computation-predicted, stable, and inexpensive single-atom nanocatalyst $Pt@MO_2C$—an important advanced material for H_2 production. J Mater Chem A 5:14658–14672. https://doi.org/10.1039/c7ta03115g

Liang JX, Lin J, Yang XF, Wang AQ, Qiao BT, Liu J, Zhang T, Li J (2014) Theoretical and experimental investigations on single-atom catalysis: Ir_1/FeO x for Co oxidation. J Phys Chem C 118:21945–21951. https://doi.org/10.1021/jp503769d

Liang S, Hao C, Shi Y (2015) The power of single-atom catalysis. ChemCatChem 7:2559–2567. https://doi.org/10.1002/cctc.201500363

Liang JX, Yang XF, Wang A, Zhang T, Li J (2016) Theoretical investigations of non-noble metal single-atom catalysis: Ni_1/FeO_x

for co oxidation. Catal Sci Technol 6:6886–6892. https://doi.org/10.1039/c6cy00672h

Liang JX, Wang YG, Yang XF, Xing DH, Wang AQ, Zhang T, Li J (2017a) Recent advances in single-atom catalysis. Encycl Inorg Bioinorg Chem. https://doi.org/10.1002/9781119951438.eibc2448

Liang S, Qiao B, Song X, Hao C, Wang A, Zhang T, Shi Y (2017b) Experimental investigation and theoretical exploration of single-atom electrocatalysis in hybrid photovoltaics: the powerful role of pt atoms in triiodide reduction. Nano Energy 39:1–8. https://doi.org/10.1016/j.nanoen.2017.06.036

Lin ZZ (2016) Graphdiyne-supported single-atom Sc and Ti catalysts for high-efficient CO oxidation. Carbon 108:343–350. https://doi.org/10.1016/j.carbon.2016.07.040

Lin J, Qiao B, Liu J, Huang Y, Wang A, Li L, Zhang W, Allard LF, Wang X, Zhang T (2012) Design of a highly active Ir/Fe(OH)$_x$ catalyst: versatile application of Pt-group metals for the preferential oxidation of carbon monoxide. Angew Chem Int Ed 51:2920–2924. https://doi.org/10.1002/anie.201106702

Lin J, Wang A, Qiao B, Liu X, Yang X, Wang X, Liang J, Li J, Liu J, Zhang T (2013a) Remarkable performance of Ir_1/FeO_x single-atom catalyst in water gas shift reaction. J Am Chem Soc 135:15314–15317. https://doi.org/10.1021/ja408574m

Lin S, Ye X, Johnson RS, Guo H (2013b) First-principles investigations of metal (Cu, Ag, Au, Pt, Rh, Pd, Fe Co, and Ir) doped hexagonal boron nitride nanosheets: stability and catalysis of Co oxidation. J Phys Chem C 117:17319–17326. https://doi.org/10.1021/jp4055445

Lin J, Qiao B, Li N, Li L, Sun X, Liu J, Wang X, Zhang T (2015) Little do more: a highly effective Pt_1/FeO_x single-atom catalyst for the reduction of no by H_2. Chem Commun 51:7911–7914. https://doi.org/10.1039/c5cc00714c

Liqiong W, Feng L, Simin L, Yuhua W, Haijun Z (2017) Preparation, characterization and catalytic performance of single-atom catalysts. Chin J Catal 38:1528–1539. https://doi.org/10.1016/S1872-2067(17)62770-0

Liu J (2017) Catalysis by supported single metal atoms. ACS Catal 7:34–59. https://doi.org/10.1021/acscatal.6b01534

Liu H, Wang C (2014) Luminescent Cu(0)@Cu(i)–TGA core–shell nanoclusters via self-assembly. Synth Met 198:329–334. https://doi.org/10.1016/j.synthmet.2014.10.044

Liu X, Duan T, Sui Y, Meng C, Han Y (2014) Copper atoms embedded in hexagonal boron nitride as potential catalysts for CO oxidation: a first-principles investigation. RSC Adv 4:38750–38760. https://doi.org/10.1039/c4ra06436d

Liu X, Duan T, Meng C, Han Y (2015) Pt atoms stabilized on hexagonal boron nitride as efficient single-atom catalysts for CO oxidation: a first-principles investigation. RSC Adv 5:10452–10459. https://doi.org/10.1039/c4ra14482a

Liu J, Lucci FR, Yang M, Lee S, Marcinkowski MD, Therrien AJ, Williams CT, Sykes EC, Flytzani-Stephanopoulos M (2016a) Tackling CO poisoning with single-atom alloy catalysts. J Am Chem Soc 138:6396–6399. https://doi.org/10.1021/jacs.6b03339

Liu W, Zhang L, Yan W, Liu X, Yang X, Miao S, Wang W, Wang A, Zhang T (2016b) Single-atom dispersed Co–N–C catalyst: structure identification and performance for hydrogenative coupling of nitroarenes. Chem Sci 7:5758–5764. https://doi.org/10.1039/c6sc02105k

Liu J, Matthew DM, Colin JM, Melissa LL, Natalie AW, Felicia RL, Maria F, Charles HS (2017a) Selective formic acid dehydrogenation on Pt–Cu single-atom alloys. ACS Catal 7:413–420. https://doi.org/10.1021/acscatal.6b02772

Liu JC, Wang YG, Li J (2017b) Toward rational design of oxide-supported single-atom catalysts: atomic dispersion of gold on ceria. J Am Chem Soc 139:6190–6199. https://doi.org/10.1021/jacs.7b01602

Liu Z, He T, Liu K, Chen W, Tang Y (2017c) Structural, electronic and catalytic performances of single-atom Fe stabilized by divacancy-nitrogen-doped graphene. RSC Adv 7:7920–7928. https://doi.org/10.1039/c6ra28387j

Liu W, Zhang L, Liu X, Liu X, Yang X, Miao S, Wang W, Wang A, Zhang T (2017d) Discriminating catalytically active FeN_x species of atomically dispersed Fe–N–C catalyst for selective oxidation of the C–H bond. J Am Chem Soc. https://doi.org/10.1021/jacs.7b05130

Long B, Tang Y, Li J (2016) New mechanistic pathways for co oxidation catalyzed by single-atom catalysts: supported and doped Au_1/ThO_2. Nano Res 9:3868–3880. https://doi.org/10.1007/s12274-016-1256-x

Longhua T, Yueming L, Hongbing F, Jin L, Jinghong L (2009) Preparation, structure, and electrochemical properties of reduced graphene sheet films. Adv Funct Mater 19:2782–2789. https://doi.org/10.1002/adfm.200900377

Lu J, Ceren A, Nigel DB, Bruce CG (2012) Imaging isolated gold atom catalytic sites in zeolite NaY. Angew Chem Int Ed 51:5842–5846. https://doi.org/10.1002/anie.201107391

Lu Z, Lv P, Yang Z, Li S, Ma D, Wu R (2017) A promising single atom catalyst for CO oxidation: Ag on boron vacancies of h-BN sheets. Phys Chem Chem Phys 19:16795–16805. https://doi.org/10.1039/c7cp02430d

Lucci FR, Liu J, Marcinkowski MD, Yang M, Allard LF, Flytzani-Stephanopoulos M, Sykes ECH (2015) Selective hydrogenation of 1,3-butadiene on platinum–copper alloys at the single-atom limit. Nat Commun 6:8550–8557. https://doi.org/10.1038/ncomms9550

Lucci FR, Darby MT, Mattera MF, Ivimey CJ, Therrien AJ, Michaelides A, Stamatakis M, Sykes EC (2016) Controlling hydrogen activation, spillover, and desorption with Pd–Au single-atom alloys. J Phys Chem. Lett 7:480–485. https://doi.org/10.1021/acs.jpclett.5b02400

Ma X, Lv Y, Xu J, Liu Y, Zhang R, Zhu Y (2012) A strategy of enhancing the photoactivity of g-C_3N_4 via doping of nonmetal elements: a first-principles study. J Phys Chem C 116:23485–23493. https://doi.org/10.1021/jp308334x

Ma DW, Li T, Wang Q, Yang G, He C, Ma B, Lu Z (2015) Graphyne as a promising substrate for the noble-metal single-atom catalysts. Carbon 95:756–765. https://doi.org/10.1016/j.carbon.2015.09.008

Ma DW, Wang Q, Yan X, Zhang X, He C, Zhou D, Tang Y, Lu Z, Yang Z (2016) 3d transition metal embedded C_2N monolayers as promising single-atom catalysts: a first-principles study. Carbon 105:463–473. https://doi.org/10.1016/j.carbon.2016.04.059

Machado BF, Serp P (2012) Graphene-based materials for catalysis. Catal Sci Technol 2:54–75. https://doi.org/10.1039/c1cy00361e

Mao K, Li L, Zhang W, Pei Y, Zeng XC, Wu X, Yang J (2014) A theoretical study of single-atom catalysis of CO oxidation using Au embedded 2d h-BN monolayer: a co-promoted O_2 activation. Sci Rep 4:5441–5447. https://doi.org/10.1038/srep05441

Mark T, Vladimir BG, Owain PHV, Pavel A, Angel BM, Mintcho ST, Brian FGJ, Richard ML (2008) Selective oxidation with dioxygen by gold nanoparticle catalysts derived from 55-atom clusters. Nature 454:981–983. https://doi.org/10.1038/nature07194

Matsubu JC, Yang VN, Christopher P (2015) Isolated metal active site concentration and stability control catalytic CO_2 reduction selectivity. J Am Chem Soc 137:3076–3084. https://doi.org/10.1021/ja5128133

Matthew JK, Phillip C (2016) Utilizing quantitative in situ FTIR spectroscopy to identify well-coordinated Pt atoms as the active site for CO oxidation on Al_2O_3-supported pt catalysts. ACS Catal 6:5599–5609. https://doi.org/10.1021/acscatal.6b01128

Melanie M, Mina Y, Lawrence FA, David RM, Wu Z, Yang X, Gabriel V, Stocks GM, Chaitanya KN (2013) Co oxidation on supported

single Pt atoms: experimental and ab initio density functional studies of CO interaction with Pt atom on θ-Al_2O_3(010) surface. J Am Chem Soc 135:12634–12645. https://doi.org/10.1021/ja401847c

Ming Y, Sha L, Yuan W, Jeffrey AH, Ye X, Lawrence FA, Sungsik L, Jun H, Manos M, Maria F (2014) Catalytically active Au–O(OH)$_x$-species stabilized by alkali ions on zeolites and mesoporous oxides. Science 346:1498–1501. https://doi.org/10.1126/science.1260526

Mykola T, Pingo M, Martin O, Prokop H, Francois CB, Jindrich K, Martin V, Pavel J, Martin S (2014) Achieving high-quality single-atom nitrogen doping of graphene/SiC(0001) by ion implantation and subsequent thermal stabilization. ACS Nano 8:7318–7324. https://doi.org/10.1021/nn502438k

Narula CK, Stocks GM (2012) Ab initio density functional calculations of adsorption of transition metal atoms on θ-Al_2O_3(010) surface. J Phys Chem C 116:5628–5636. https://doi.org/10.1021/jp209725a

Narula CK, Allard LF, Stocks GM, Moses-Debusk M (2014) Remarkable no oxidation on single supported platinum atoms. Sci Rep 4:7238. https://doi.org/10.1038/srep07238

Neitzel A, Figueroba A, Lykhach Y, Skála T, Vorokhta M, Tsud N, Mehl S, Ševčíková K, Prince KC, Neyman KM, Matolín V, Libuda J (2016) Atomically dispersed Pd, Ni, and Pt species in ceria-based catalysts: principal differences in stability and reactivity. J Phys Chem C 120:9852–9862. https://doi.org/10.1021/acs.jpcc.6b02264

Ogino I (2017) X-ray absorption spectroscopy for single-atom catalysts: critical importance and persistent challenges. Chin J Catal 38:1481–1488. https://doi.org/10.1016/S1872-2067(17)62880-8

Parkinson GS (2017) Unravelling single atom catalysis: the surface science approach. Chin J Catal 38:1454–1459. https://doi.org/10.1016/S1872-2067(17)62878-X

Pei GX, Liu XY, Wang A, Li L, Huang Y, Zhang T, Lee JW, Jang BWL, Mou CY (2014) Promotional effect of Pd single atoms on Au nanoparticles supported on silica for the selective hydrogenation of acetylene in excess ethylene. New J Chem 38:2043–2051. https://doi.org/10.1039/c3nj01136d

Pengxin L, Yun Z, Ruixuan Q, Shiguang M, Guangxu C, Lin G, Daniel MC, Peng Z, Qing G, Dandan Z, Binghui W, Gang F, Nanfeng Z (2016) Photochemical route for synthesizing atomically dispersed palladium catalysts. Science 352:797–802. https://doi.org/10.1126/science.aaf5251

Peterson EJ, Delariva AT, Lin S, Johnson RS, Guo H, Miller JT, Hun Kwak J, Peden CH, Kiefer B, Allard LF, Ribeiro FH, Datye AK (2014) Low-temperature carbon monoxide oxidation catalysed by regenerable atomically dispersed palladium on alumina. Nat Commun 5:4885–4895. https://doi.org/10.1038/ncomms5885

Piernavieja-Hermida M, Lu Z, White A, Low K-B, Wu T, Elam JW, Wu Z, Lei Y (2016) Towards ALD thin film stabilized single-atom Pd_1 catalysts. Nanoscale 8:15348–15356. https://doi.org/10.1039/c6nr04403d

Ping S, Xiaozhi L, Wei X, Weilin X, Zheng J, Lin G (2017) Zn single atom catalyst for highly efficient oxygen reduction reaction. Adv Funct Mater 27:1700802. https://doi.org/10.1002/adfm.201700802

Pingping H, Zhiwei H, Zakariae A, Michiel M, Fei X, Freek K, Alla D, Yaxin C, Xiao G, Xingfu T (2014) Electronic metal-support interactions in single-atom catalysts. Angew Chem Int Ed 53:3418–3421. https://doi.org/10.1002/anie.201309248

Qiao Wang A, Yang X, Lawrence FA, Zheng J, Cui Y, Liu J, Jun L, Zhang T (2011) Single-atom catalysis of CO oxidation using Pt_1/FeO_x. Nat Chem 3:634–641. https://doi.org/10.1038/nchem.1095

Qiao B, Lin J, Wang A, Chen Y, Zhang T, Liu J (2015a) Highly active Au_1/Co_3O_4 single-atom catalyst for CO oxidation at room temperature. Chin J Catal 36:1505–1511. https://doi.org/10.1016/s1872-2067(15)60889-0

Qiao B, Liang JX, Wang A, Xu CQ, Li J, Zhang T, Liu JJ (2015b) Ultrastable single-atom gold catalysts with strong covalent metal-support interaction (CMSI). Nano Res 8:2913–2924. https://doi.org/10.1007/s12274-015-0796-9

Qiu HJ, Ito Y, Cong W, Tan Y, Liu P, Hirata A, Fujita T, Tang Z, Chen M (2015) Nanoporous graphene with single-atom nickel dopants: an efficient and stable catalyst for electrochemical hydrogen production. Angew Chem Int Ed Engl 54:14031–14035. https://doi.org/10.1002/anie.201507381

Rosa A, Zailai X, Youngmi Y, Gregor W, Li LS, Klaus EH, Matthias F, Patrick K, Michael H, Axel KG, Robert S (2015) Nature of the N–Pd interaction in nitrogen-doped carbon nanotube catalysts. ACS Catal 5:2740–2753. https://doi.org/10.1021/acscatal.5b00094

Sakthivel S, Shankar MV, Palanichamy M, Banumathi A, Bahnemann DW, Murugesan V (2004) Enhancement of photocatalytic activity by metal deposition: characterisation and photonic efficiency of Pt, Au and Pd deposited on TiO_2 catalyst. Water Res 38:3001–3008. https://doi.org/10.1016/j.watres.2004.04.046

Salai CA, Andreas H (2017) Water–gas shift activity of atomically dispersed cationic platinum versus metallic platinum clusters on titania supports. ACS Catal 7:301–309. https://doi.org/10.1021/acscatal.6b02764

Sara A, Salai CA, Andreas H (2014) On the importance of metal–oxide interface sites for the water–gas shift reaction over Pt/CeO_2 catalysts. J Catal 309:314–324. https://doi.org/10.1016/j.jcat.2013.10.012

Seoin B, Yousung J (2017) TiC- and TiN-supported single-atom catalysts for dramatic improvements in CO_2 electrochemical reduction to CH_4. ACS Energy Lett 2:969–975. https://doi.org/10.1021/acsenergylett.7b00152

Shapovalov V, Metiu H (2007) Catalysis by doped oxides: Co oxidation by $Au_xCe_{1-x}O_2$. J Catal 245:205–214. https://doi.org/10.1016/j.jcat.2006.10.009

Shi J (2017) Single-atom Co-doped MoS_2 monolayers for highly active biomass hydrodeoxygenation. Chem 2:468–469. https://doi.org/10.1016/j.chempr.2017.03.005

Shi JL, Wu JH, Zhao XJ, Xue XL, Gao YF, Guo ZX, Li SF (2016) Substrate Co-doping modulates electronic metal-support interactions and significantly enhances single-atom catalysis. Nanoscale 8:19256–19262. https://doi.org/10.1039/c6nr04292a

Simon FJH, Rik MB, Mhairi HG, Ian H, Andrew DN, Karen W, Adam FL (2007) High-activity, single-site mesoporous Pd/Al_2O_3 catalysts for selective aerobic oxidation of allylic alcohols. Angew Chem 119:8747–8750. https://doi.org/10.1002/ange.200702534

Song W, Hensen EJM (2013) Structure sensitivity in CO oxidation by a single au atom supported on ceria. J Phys Chem C 117:7721–7726. https://doi.org/10.1021/jp400977m

Song W, Jansen APJ, Hensen EJM (2013) A computational study of the influence of the ceria surface termination on the mechanism of CO oxidation of isolated Rh atoms. Faraday Discuss 162:281. https://doi.org/10.1039/c3fd20129e

Songhai X, Wataru K, Yuichi N, Tatsuya T (2012) Enhancement in aerobic alcohol oxidation catalysis of Au_{25} clusters by single Pd atom doping. ACS Catal 2:1519–1523. https://doi.org/10.1021/cs300252g

Stambula S, Gauquelin N, Bugnet M, Gorantla S, Turner S, Sun S, Liu J, Zhang G, Sun X, Botton GA (2014) Chemical structure of nitrogen-doped graphene with single platinum atoms and atomic clusters as a platform for the PEMFC electrode. J Phys Chem C 118:3890–3900. https://doi.org/10.1021/jp408979h

Strizhak PE (2013) Nanosize effects in heterogeneous catalysis. Theor Exp Chem 49:2–21. https://doi.org/10.1007/s11237-013-9297-7

Sun S, Zhang G, Nicolas G, Ning C, Zhou J, Yang S, Chen W, Meng X, Geng D, Mohammad NB, Ruying L, Ye S, Shanna K, Gianluigi AB, Sham T, Sun X (2013) Single-atom catalysis using Pt/graphene achieved through atomic layer deposition. Sci Rep 3(2013):1775–1783. https://doi.org/10.1038/srep01775

Sun X, Lin J, Zhou Y, Li L, Su Y, Wang X, Zhang T (2017) Feox supported single-atom pd bifunctional catalyst for water gas shift reaction. AIChE J 63:4022–4031. https://doi.org/10.1002/aic.15759

Sungeun Y, Hyunjoo L (2013) Atomically dispersed platinum on gold nano-octahedra with high catalytic activity on formic acid oxidation. ACS Catal 3:437–443. https://doi.org/10.1021/cs300809j

Sungeun Y, Jiwhan K, Young JT, Aloysius S, Hyunjoo L (2016) Single-atom catalyst of platinum supported on titanium nitride for selective electrochemical reactions. Angew Chem Int Ed 55:2058–2062. https://doi.org/10.1002/anie.201509241

Sungeun Y, Jiwhan K, Aloysius S, Hyunjoo L (2017) Support effects in single-atom platinum catalysts for electrochemical oxygen reduction. ACS Catal 7:1301–1307. https://doi.org/10.1021/acscatal.6b02899

Tang Y, Zhao S, Long B, Liu JC, Li J (2016) On the nature of support effects of metal dioxides MO_2(m = Ti, Zr, Hf, Ce, Th) in single-atom gold catalysts: importance of quantum primogenic effect. J Phys Chem C 120:17514–17526. https://doi.org/10.1021/acs.jpcc.6b05338

Tauster SJ, Fung SC, Garten RL (1978) Strong metal-support interactions group 8 noble metals supported on TiO_2. J Am Chem Soc 100:170–175. https://doi.org/10.1021/ja00469a029

Thomas JM, Raja R, Lewis DW (2005) Single-site heterogeneous catalysts. Angew Chem Int Ed 44:6456–6482. https://doi.org/10.1002/anie.200462473

Ting D, Weitao Z, Wei Z (2017) Increasing the range of non-noble-metal single-atom catalysts. Chin J Catal 38:1489–1497. https://doi.org/10.1016/S1872-2067(17)62799-2

Wang H, Wang Q, Cheng Y, Li K, Yao Y, Zhang Q, Dong C, Wang P, Schwingenschlögl U, Yang W, Zhang XX (2012) Doping monolayer graphene with single atom substitutions. Nano Lett 12:141–144. https://doi.org/10.1021/nl2031629

Wang Z, Hao X, Gerhold S, Mares P, Wagner M, Bliem R, Schulte K, Schmid M, Franchini C, Diebold U (2014a) Stabilizing single Ni adatoms on a two-dimensional porous titania overlayer at the $SrTiO_3$(110) surface. J Phys Chem C 118:19904–19909. https://doi.org/10.1021/jp506234r

Wang WL, Santos EJG, Jiang B, Cubuk ED, Ophus C, Centeno A, Pesquera A, Zurutuza A, Ciston J, Westervelt R, Kaxiras E (2014b) Direct observation of a long-lived single-atom catalyst chiseling atomic structures in graphene. Nano Lett 14:450–455. https://doi.org/10.1021/nl403327u

Wang Y, Yuan H, Li Y, Chen Z (2015a) Two-dimensional iron-phthalocyanine (Fe-PC) monolayer as a promising single-atom-catalyst for oxygen reduction reaction: a computational study. Nanoscale 7:11633–11641. https://doi.org/10.1039/c5nr00302d

Wang YG, Mei D, Glezakou VA, Li J, Rousseau R (2015b) Dynamic formation of single-atom catalytic active sites on ceria-supported gold nanoparticles. Nat Commun 6:6511–6518. https://doi.org/10.1038/ncomms7511

Wang Z, Zang L, Fan X, Jia H, Li L, Deng W, Wang C (2015c) Defect-mediated of Cu@TiO_2 core-shell nanoparticles with oxygen vacancies for photocatalytic degradation 2,4-DCP under visible light irradiation. Appl Surf Sci 358:479–484. https://doi.org/10.1016/j.apsusc.2015.08.051

Wang L, Zhang W, Wang S, Gao Z, Luo Z, Wang X, Zeng R, Li A, Li H, Wang M, Zheng X, Zhu J, Zhang W, Ma C, Si R, Zeng J (2016a) Atomic-level insights in optimizing reaction paths for hydroformylation reaction over Rh/CoO single-atom catalyst. Nat Commun 7:14036–14043. https://doi.org/10.1038/ncomms14036

Wang J, Zhao X, Lei N, Li L, Zhang L, Xu S, Miao S, Pan X, Wang A, Zhang T (2016b) Hydrogenolysis of glycerol to 1,3-propanediol under low hydrogen pressure over WO_x-supported single/pseudo-single atom pt catalyst. ChemSusChem 9:784–790. https://doi.org/10.1002/cssc.201501506

Wang ZT, Darby MT, Therrien AJ, El-Soda M, Michaelides A, Stamatakis M, Sykes ECH (2016c) Preparation, structure, and surface chemistry of Ni–Au single atom alloys. J Phys Chem C 120:13574–13580. https://doi.org/10.1021/acs.jpcc.6b03473

Wei X, Yang XF, Wang AQ, Li L, Liu XY, Zhang T, Mou CY, Li J (2012) Bimetallic Au–Pd alloy catalysts for N_2O decomposition: effects of surface structures on catalytic activity. J Phys Chem C 116:6222–6232. https://doi.org/10.1021/jp210555s

Wei H, Liu X, Wang A, Zhang L, Qiao B, Yang X, Huang Y, Miao S, Liu J, Zhang T (2014) Feox-supported platinum single-atom and pseudo-single-atom catalysts for chemoselective hydrogenation of functionalized nitroarenes. Nat Commun 5:5634–5641. https://doi.org/10.1038/ncomms6634

Wu P, Du P, Zhang H, Cai C (2015) Graphyne-supported single fe atom catalysts for CO oxidation. Phys Chem Chem Phys 17:1441–1449. https://doi.org/10.1039/c4cp04181j

Xiang-Kui G, Botao Q, Chuan-Qi H, Wu-Chen D, Keju S, Ensheng Z, Tao Z, Jingyue L, Wei-Xue L (2014) Supported single Pt_1/Au_1 atoms for methanol steam reforming. ACS Catal 4:3886–3890. https://doi.org/10.1021/cs500740u

Xiaogang L, Wentuan B, Lei Z, Shi T, Wangsheng C, Qun Z, Yi L, Changzheng W, Yi X (2016) Single-atom Pt as co-catalyst for enhanced photocatalytic H_2 evolution. Adv Mater 28:2427–2431. https://doi.org/10.1002/adma.201505281

Xin-Bo Z, Jun-Min Y, Song H, Hiroshi S, Qiang X (2009) Magnetically recyclable Fe@Pt core-shell nanoparticles and their use as electrocatalysts for ammonia borane oxidation: the role of crystallinity of the core. J Am Chem Soc 131:2778–2779. https://doi.org/10.1021/ja808830a

Xing J, Chen JF, Li YH, Yuan WT, Zhou Y, Zheng LR, Wang HF, Hu P, Wang Y, Zhao HJ, Wang Y, Yang HG (2014) Stable isolated metal atoms as active sites for photocatalytic hydrogen evolution. Chem Eur J 20:2138–2144. https://doi.org/10.1002/chem.201303366

Xinjiang C, Xingchao D, Carsten K, Marga-Martina P, Sebastian W, Feng S, Angelika B, Matthias B (2017) Synthesis of single atom based heterogeneous platinum catalysts: high selectivity and activity for hydrosilylation reactions. ACS Cent Sci 3:580–585. https://doi.org/10.1021/acscentsci.7b00105

Xu G, Wang R, Yang F, Ma D, Yang Z, Lu Z (2017) CO oxidation on single Pd atom embedded defect-graphene via a new termolecular Eley–Rideal mechanism. Carbon 118:35–42. https://doi.org/10.1016/j.carbon.2017.03.034

Yan T, Jin-Xia L, Jun L (2017a) Investigation of water adsorption and dissociation on Au_1/CeO_2 single-atom catalysts using density functional theory. Chin J Catal 38:1558–1565. https://doi.org/10.1016/S1872-2067(17)62829-8

Yan T, Yang-Gang W, Jun L (2017b) Theoretical investigations of Pt_1@CeO_2 single-atom catalyst for CO oxidation. J Phys Chem C 121:11281–11289. https://doi.org/10.1021/acs.jpcc.7b00313

Yang M, Flytzani-Stephanopoulos M (2017) Design of single-atom metal catalysts on various supports for the low-temperature water–gas shift reaction. Catal Today. https://doi.org/10.1016/j.cattod.2017.04.034

Yang L, Jingyue L (2017) Co oxidation on metal oxide supported single Pt atoms: the role of the support. Ind Eng Chem Res 56:6916–6925. https://doi.org/10.1021/acs.iecr.7b01477

Yang T, Tetsu T (2005) Mechanisms and applications of plasmon-induced charge separation at TiO_2 films loaded with gold nanoparticles. J Am Chem Soc 127:7632–7637. https://doi.org/10.1021/ja042192u

Yang M, Allard LF, Flytzani-Stephanopoulos M (2013a) Atomically dispersed Au–(OH)_ species bound on titania catalyze the low-temperature water–gas shift reaction. J Am Chem Soc 135:3768–3771. https://doi.org/10.1021/ja312646d

Yang XF, Aiqin W, Botao Q, Jun L, Jingyue L, Tao Z (2013b) Single-atom catalysts: a new frontier in heterogeneous catalysis. Acc Chem Res 46:1740–1748. https://doi.org/10.1021/ar300361m

Yang M, Liu J, Lee S, Zugic B, Huang J, Allard LF, Flytzani-Stephanopoulos M (2015) A common single-site Pt(ii)–O(OH)$_x$-species stabilized by sodium on "active" and "inert" supports catalyzes the water–gas shift reaction. J Am Chem Soc 137:3470–3473. https://doi.org/10.1021/ja513292k

Yang T, Fukuda R, Hosokawa S, Tanaka T, Sakaki S, Ehara M (2017) A theoretical investigation on CO oxidation by single-atom catalysts M_1/γ-Al_2O_3 (m = Pd, Fe Co, and Ni). ChemCatChem 9:1222–1229. https://doi.org/10.1002/cctc.201601713

Yantao S, Haisheng W, Jiahao G, Suxia L, Aiqin W, Tao Z, Jingyue L, Tingli M (2014) Single-atom catalysis in mesoporous photovoltaics: the principle of utility maximization. Adv Mater 26:8147–8153. https://doi.org/10.1002/adma.201402978

Yong W, Weitao Z, Dehui D, Xinhe B (2017) Two-dimensional materials confining single atoms for catalysis. Chin J Catal 38:1443–1453. https://doi.org/10.1016/S1872-2067(17)62839-0

Zhang X, Shi H, Xu BQ (2005) Catalysis by gold: isolated surface Au^{3+} ions are active sites for selective hydrogenation of 1,3-butadiene over Au/ZrO_2 catalysts. Angew Chem Int Ed 44:7132–7135. https://doi.org/10.1002/anie.200502101

Zhang H, Tatsuya W, Mitsutaka O, Masatake H, Naoki T (2011) Catalytically highly active top gold atom on palladium nanocluster. Nat Mater 11:49–52. https://doi.org/10.1038/nmat3143

Zhang RQ, Lee TH, Yu BD, Stampfl Soon A (2012a) The role of titanium nitride supports for single-atom platinum-based catalysts in fuel cell technology. Phys Chem Chem Phys 14:16552–16557. https://doi.org/10.1039/c2cp41392b

Zhang W, Xu S, Han X, Bao X (2012b) In situ solid-state NMR for heterogeneous catalysis: a joint experimental and theoretical approach. Chem Soc Rev 41:192–210. https://doi.org/10.1039/c1cs15009j

Zhang X, Guo J, Guan P, Liu C, Huang H, Xue F, Dong X, Pennycook SJ, Chisholm MF (2013) Catalytically active single-atom niobium in graphitic layers. Nat Commun 4:1924–1930. https://doi.org/10.1038/ncomms2929

Zhang H, Kawashima K, Okumura M, Toshima N (2014) Colloidal Au single-atom catalysts embedded on Pd nanoclusters. J Mater Chem A 2:13498–13508. https://doi.org/10.1039/c4ta01696c

Zhang X, Lei J, Wu D, Zhao X, Jing Y, Zhou Z (2016a) A Ti-anchored Ti_2CO_2 monolayer (MXene) as a single-atom catalyst for co oxidation. J Mater Chem A 4:4871–4876. https://doi.org/10.1039/c6ta00554c

Zhang B, Asakura H, Zhang J, Zhang J, De S, Yan N (2016b) Stabilizing a platinum single-atom catalyst on supported phosphomolybdic acid without compromising hydrogenation activity. Angew Chem Int Ed 55:8319–8323. https://doi.org/10.1002/anie.201602801

Zhang H, Wei J, Dong J, Liu G, Shi L, An P, Zhao G, Kong J, Wang X, Meng X, Zhang J, Ye J (2016c) Efficient visible-light-driven carbon dioxide reduction by a single-atom implanted metal-organic framework. Angew Chem Int Ed 55:14310–14314. https://doi.org/10.1002/anie.201608597

Zhao P, Su Y, Zhang Y, Li SJ, Chen G (2011) CO catalytic oxidation on iron-embedded hexagonal boron nitride sheet. Chem Phys Lett 515:159–162. https://doi.org/10.1016/j.cplett.2011.09.034

Zhiwei H, Qingqing C, Pingping H, Jiming H, Junhua L, Xingfu T (2012) Catalytically active single-atom sites fabricated from silver particles. Angew Chem Int Ed 51:4198–4203. https://doi.org/10.1002/anie.201109065

Zhou S, Duan Y, Wang F, Wang C (2017) Fluorescent au nanoclusters stabilized by silane: facile synthesis, color-tunability and photocatalytic properties. Nanoscale 9:4981–4988. https://doi.org/10.1039/c7nr01052d

Zhu C, Fu S, Shi Q, Du D, Lin Y (2017) Single-atom electrocatalysts. Angew Chem Int Ed. https://doi.org/10.1002/anie.201703864

Zupeng C, Sharon MEV, Rowan KL, Roland H, Tom F, Quentin MR, John MT, Paul AM, Dariya D, Markus A, Sergey P, Núria L, Javier PR (2017) Stabilization of single metal atoms on graphitic carbon nitride. Adv Funct Mater 27:1605785–1605796. https://doi.org/10.1002/adfm.201605785